July 31, 2014

Thermodynamic Evaluations Progress Report M4FT-14LL0806039

M. Zavarin[a], A. Benedicto[b], A.B. Kersting[a], and M. Sutton[c]

[a]Glenn T. Seaborg Institute, Physical & Life Sciences, Lawrence Livermore National Laboratory, 7000 East Avenue, Livermore, CA 94550, USA.
[b]CIEMAT, Department of Environment, Avenida Complutense, 40, 28040 Madrid, Spain.
[c]Global Security, Lawrence Livermore National Laboratory, 7000 East Avenue, Livermore, CA 94550, USA.

DISCLAIMER

Contents

1. Introduction

This progress report (Milestone Number M4FT-13LL0806039) summarizes research conducted at LLNL within Work Package Number FT-13LL080603. The focus of this research is the thermodynamic modeling of EBS materials and properties and development of thermodynamic databases and models to evaluate the stability of EBS materials and their interactions with fluids at various physico-chemical conditions relevant to subsurface repository environments. The development and implementation of equilibrium thermodynamic models are intended to describe chemical and physical processes such as solubility, sorption, and diffusion.

Thermodynamic data are essential for understanding and evaluating geochemical processes, such as speciation-solubility, reaction-paths, or reactive transport. The data are required to evaluate both equilibrium states and the kinetic approach to such states. However, thermodynamic databases are often limited and do not span the range of conditions that may be exist under the various generic repository scenarios (salt, deep borehole, etc.). For example, previously developed thermodynamic data overstate the stabilities of smectites and illites. While this was adequate for both tuff and salt host rock, the databases have some deficiencies with respect to other repository designs such as those in clay/shale, or those that include a clay/bentonite buffer. Data that continue to come out of the NEA review program were not incorporated into the previous DOE thermodynamic databases. However, NEA data are also limited and do not account for pressure extrapolations applicable for deep borehole repositories. Ion exchange data and surface complexation processes are also lacking in most current thermodynamic databases.

The existing thermodynamic database development task is a continuation of a FY13 effort. This task includes revising the previously developed thermodynamic databases and expanding them to cover the needs of the repository types currently under consideration by the UFD (i.e. clay, granite, deep borehole). This effort is focused on developing data and models for clays. The effort is a collaboration between LLNL and SNL. A second task includes participation of Cynthia Atkins-Duffin (LLNL) in the NEA Thermodynamic Database (TDB) program. A third task involves a collaboration with Dr. V. Brendler (Dresden-Rossendorf) focused on the development of thermodynamic databases for high ionic strength conditions as well as surface complexation modeling. The fourth task is a recently completed study of Np interaction with clay, looking at the effect of solution chemistry on ion exchange processes. Progress made on each of these tasks is documented in the following sections.

2. Thermodynamic Database Development

A report by Wolery and Sutton (2013) identified the current state of the YMP and other thermodynamic database efforts (national and international) and identified key gaps and weaknesses in these databases. Recommendations for future database development efforts were identified. They included the following (from Wolery and Sutton, 2013):

- Continue evaluation of a large body of historical data reported over the last century
- Future database should use NEA-TBD data where feasible (post-Nickel volume)
- Consider Barin and Platzki a source of thermodynamic data to backfill NEA-TBD gaps
- Perform experiments to populate unknown data and resolve discrepancies only when absolutely required
- Establish key data for aluminum using Gibbs energy or enthalpy of corundum (Al2O3) to resolve discrepancies between Helgeson (1978) and Robie/Hemingway (1995), also incorporating Holland/Powell (1985) data
- Update SUPCRT92 mineral data for consistency with desired key data
- Maybe replace the SUPCRT92 mineral data with the Holland and Powell (2011) data, adjusting for consistency with the desired key data
- Put the SUPCRT92 functionality for calculating thermodynamic properties as a function of temperature and pressure into Cantera
- Collaborate with European investigators (Thereda, Pitzer, benchmarking)
- Fully update working databases at opportune times (e.g., do official releases)
- Take another look at temperature and pressure extrapolation of data for aqueous species for which HKF EOS data are not available
- Address high-ionic strength model data (Pitzer model, others)
- Include surface complexation modeling improvements as well as chemical thermodynamic data improvements

[References: (Helgeson et al., 1978; Holland and Powell, 1985; Holland and Powell, 2011; Powell and Holland, 1985; Robie and Hemingway, 1995)]

Progress has been made on some of these items. For example, LLNL is actively supporting the NEA-TDB effort which is the most active international database development project. The most recent NEA-TDB publication is the first of two volumes summarizing the thermodynamics of iron (Lemire et al., 2013). We have also been following the development progress of the THEREDA database effort. The most recent 9th data release included parameter files for the system Na, K, Mg-Ca-Cl-SO4-HCO_3/CO_2(g)-Si-U(IV)/U(VI)-H_2O. Importantly, the THEREDA effort is focused on a Pitzer model which is most relevant to high ionic strengths prevalent in salt rock repositories and other disposal scenarios. The THEREDA database project continues to support the EQ3/6 modeling code database format. Development of surface complexation modeling databases was supported through discussions with the RES^{3}T development group. These are highlighted in Section 3 of this document.

3. Comprehensive Approaches to Developing Ion Exchange and Surface Complexation Models for Nuclear Waste Repository Conditions

The need to develop self-consistent surface complexation/ion exchange models, in concert with thermodynamic models, for nuclear waste repository performance assessment was identified many years ago (Bradbury and Baeyens, 1993). This issue was expressly identified in the recent NEA Sorption project reports (Davis et al., 2005; Ochs et al., 2012). However, significant progress on this issue has been made only recently in various international nuclear waste repository programs (e.g. (Bradbury and Baeyens, 2009), (Dresden-Rossendorf, 2013), (Geckeis et al., 2013)). Hybrid approaches have also been attempted (Bradbury et al., 2010). The best path forward for developing such databases remains an open question (Geckeis et al., 2013), particularly in cases where generic repositories are being investigated resulting in a need to model radionuclide behavior over a very broad range of solution and mineralogic conditions.

One promising effort underway in Germany is the development of an open source database of surface complexation constants reported in the open literature (Dresden-Rossendorf, 2013). RES³T is a digital open source thermodynamic sorption database. It is mineral-specific and can therefore also be used for additive models of more complex solid phases such as rocks or soils. The database includes an integrated user interface to access selected mineral and sorption data and export data into formats suitable for other modeling software. Data records comprise mineral properties, specific surface areas, characteristics of surface binding sites and their protolysis, sorption ligand information, and surface complexation reactions. The database includes the following surface complexation models: Non-Electrostatic, Diffuse Double Layer, Constant Capacitance, Triple Layer, Basic Stern, and the 1-pK Model as extended to CD-MUSIC. The concept of strong and weak binding sites is also included. An extensive bibliography is included in the database, providing links to the original publications, but also to background information concerning surface complexation model theories, related software for data processing and modeling, and sorption experiment techniques. The intent of the database is to substitute the present Kd approach in risk assessment studies to the more realistic description of sorption phenomena with SCM. The RES³T approach represents the first international attempt to produce a digital thermodynamic database for surface complexation equilibria from the vast amount of data available in the literature. Recent improvement include automated conversion of reaction constants to zero ionic strength for use in surface complexation models. In addition, all database records are identified with a Digital Object Identifier (DOI) that provides a direct link to the original reference. An example database output for U(VI) sorption to quartz is reported in Table 1.

One significant difficulty in directly utilizing reaction constants supplied in the RES^{3}T database is that reported constants are dependent on the specific surface complexation model used in the referenced manuscript and the associated protonation/deprotonation constants, surface areas, site densities, and associated aqueous speciation constants and activity correction methods (e.g. Table 1). For example, reaction constants reported for U(VI) sorption to quartz are based on three different models (Diffuse Double Layer, Non-electrostatic, and Triple Layer models). A present, there is no mechanisms by which these three models can be reconciled. Moreover, within the DDL model constants, five unique surface protonation/deprotonation models are used for the quartz surface and three different surface site densities. Lastly, the choice of surface species used to fit sorption data varies; a total of seven different surface species were identified in the DDL models alone (Table 1). An additional underlying issue associated with the application of these reaction constants is that they were developed in conjunction with aqueous speciation databases available at the time of model development. As aqueous speciation databases have changed and hopefully improved with time, a mechanism by which the surface complexation constants can be updated to provide consistency with the latest aqueous speciation databases does not exist. As a result, integration of the different surface complexation models, different parameter choices, and different surface species is not straightforward. The inconsistent application of surface complexation models in the literature limits our ability to develop self-consistent databases that would be directly applicable to reactive transport modeling efforts.

One potential remedy to this situations would be for the RES^{3}T database to be expanded and store raw sorption data from which one could develop surface complexation reaction constants based on preferred SCM modeling approaches and most up to date aqueous speciation databases. UFD program at LLNL is actively engaged with the RES^{3}T group to evaluate options for a next generation RES^{3}T database that would include such raw data. A demonstration project is underway at HZDR and will be presented in a special session on Environmental Radiochemistry

at the 248th ACS National Meeting, San Francisco, California, August 10-14, 2014. This session is being organized by Don Reed, Ralph Sudowe, Brian Powell, and Mavrik Zavarin.

As a test case, we recently extracted and digitized all uranium sorption data for quartz that were reported in the RES^{3}T database (see Appendix A). The dataset amounts to approximately 500 individual sorption data points. Digitization of data allowed for simultaneous modeling off all available sorption data and the formulation of a consistent set of reactions. Furthermore, the data were fitted using the most up-to-date aqueous speciation data documents in the NEA database and accounted for the estimated uncertainty of individual data points. A statistical comparison of the data to the resulting model, based on the ratio of sorbed to aqueous U concentrations) is presented in Figure 1. The model was developed based on the simplest one-site non-electrostatic (NE) surface complexation model. Remarkably, the data were fit using only four fitting parameters: the reaction constants, K, for the species $>SiO^-$, $>SiOUO_3H$, $SiOUO_3^-$, and $SiOUO_2CO_3$. While additional evaluation of these results is still in progress, particularly with respect to testing other surface complexation modeling approached (DLM, CCM, TLM, GEM, etc.), the results show promise in our ability to develop comprehensive and self-consistent models to predict metal sorption to mineral surfaces. Figure 2 presents a comparison of measured and predicted U aqueous concentrations in each batch experiment based on the one-site NE surface complexation model fit described earlier. Again, the modeling approach used here shows remarkable promise in being able to simulated U(VI) aqueous concentrations across a very wide range of pH, ionic strength, and major ion composition. This test case provides confidence that the approach undertaken here can lead to an effective and self-consistent database of reaction constant for use in performance assessment and other nuclear waste repository risk assessments. Importantly, when compiled in a digital format, the reaction constants can be updated as aqueous speciation models evolve and our numerical models for interfacial reactions improve.

Table 1. Data extracted from RES3T database for uranium sorption to quartz.

SCM Type	Mineral	Area m2/g	Site Density nm-1	pK_1	pK_2	logK	Chemical Equation	Literature Reference
DDL	Quartz	0.2	4.81		5.62	-5.72	»Si-(OH)2 + UO2<2+> = »Si-O2-UO2 + 2 H<1+>	AZBN00a
DDL	Quartz	0.2	4.81		5.62	-5.51	»Si-(OH)2 + UO2<2+> = »Si-O2-UO2 + 2 H<1+>	AZZBN01
DDL	Quartz	10	10	-1.6	7.6	-7.259	»X-OH + UO2<2+> + H2O = »X-O-UO2(OH) + 2 H<1+>	JHLCH99
DDL	Quartz	10	10	-1.6	7.6	9.529	»X-OH + UO2<2+> + CO3<2-> = »X-O-UO2CO3<1-> + H<1+>	JHLCH99
DDL	Quartz	10	10	-1.6	7.6	-1.978	»X-OH + UO2<2+> = »X-O-UO2<1+> + H<1+>	JHLCH99
DDL	Quartz	0.05			-7.2	-16.75	»SiOH + 3 UO2<2+> + 5 H2O = »SiO-(UO2)3(OH)5 + 6 H<1+>	NB10
DDL	Quartz	0.05			-7.2	0.3	»SiOH + UO2<2+> = »SiO-UO2<1+> + H<1+>	NB10
DDL	Quartz	0.05			-7.2	-5.65	»SiOH + UO2<2+> + H2O = »SiO-UO2(OH) + 2 H<1+>	NB10
DDL	Quartz	0.31	2.3	-1.24	7.06	-0.3	»Si-OH + UO2<2+> = »Si-O-UO2<1+> + H<1+>	PJTP01
DDL	Quartz	0.31	2.3	-1.24	7.06	-18.7	»Si-OH + UO2<2+> + 3 H2O = »Si-O-UO2(OH)3<2->+ 4 H<1+>	PJTP01
DDL	Quartz	0.03	2.3		7.2	0.3	»Si-OH + UO2<2+> = »Si-O-UO2<1+> + H<1+>	PTBP98
DDL	Quartz	0.03	2.3		7.2	-16.75	»Si-OH + 3 UO2<2+> + 5 H2O = »Si-O-(UO2)3(OH)5 + 6 H<1+>	PTBP98
DDL	Quartz	0.03	2.3		7.2	-5.65	»Si-OH + UO2<2+> + H2O = »Si-O-UO2(OH) + 2 H<1+>	PTBP98
DDL	Quartz	0.1	2.31		7.2	-8.45	»Si-OH + UO2<2+> + 2 H2O = »Si-O-UO2(OH)2<1-> + 3 H<1+>	VT98
NE	Quartz	0.33	0			-4.95	»Si(w)-OH + UO2<2+> + H2O = »Si(w)-O-UO2(OH) + 2 H<1+>	DK01
NE	Quartz	0.33	0			1.06	»Si(s)-OH + UO2<2+> = »Si(s)-O-UO2<1+> + H<1+>	DK01
NE	Quartz	0.33	0			-3.19	»Si(s)-OH + UO2<2+> + H2O = »Si(s)-O-UO2(OH) + 2 H<1+>	DK01
NE	Quartz	0.33	0			-2.56	»Si(s)-OH + UO2<2+> + H2O = »Si(s)-O-UO2(OH) + 2 H<1+>	DK01
NE	Quartz	0.33	0			-4.98	»Si(w)-OH + UO2<2+> + H2O = »Si(w)-O-UO2(OH) + 2 H<1+>	DK01
NE	Quartz	0.33	0			1.2	»Si(s)-OH + UO2<2+> = »Si(s)-O-UO2<1+> + H<1+>	DK01
NE	Quartz	0.33	0			-4.64	»Si(w)-OH + UO2<2+> + H2O = »Si(w)-O-UO2(OH) + 2 H<1+>	DK01
NE	Quartz	0.33	0			-0.03	»Si(w)-OH + UO2<2+> = »Si(w)-O-UO2<1+> + H<1+>	DK01
NE	Quartz	0.33	0			-5.28	»Si(w)-OH + UO2<2+> + H2O = »Si(w)-O-UO2(OH) + 2 H<1+>	DK01
NE	Quartz	0.33	0			10.183	»Si(w)-OH + UO2<2+> + CO3<2-> = »Si(w)-O-UO2CO3<1-> + H<1+>	DK01
NE	Quartz	0.33	0			-3.28	»Si(s)-OH + UO2<2+> + H2O = »Si(s)-O-UO2(OH) + 2 H<1+>	DK01

SCM Type	Mineral	Area m2/g	Site Density nm-1	pK_1	pK_2	logK	Chemical Equation	Literature Reference
NE	Quartz	0.33	0			-4.73	»Si-OH + UO2<2+> = »Si-O-UO2(OH) + 2 H<1+>	KCKD96
NE	Quartz	0.33	0			-5.32	»Si(w)-OH + UO2<2+> + H2O = »Si(w)-O-UO2(OH) + 2 H<1+>	KCKD96
NE	Quartz	0.33	0			-2.65	»Si(s)-OH + UO2<2+> + H2O = »Si(s)-O-UO2(OH) + 2 H<1+>	KCKD96
NE	Quartz	0.33	0			-2.56	»Si(s)-O(0.5)H + UO2<2+> + H2O = »Si(s)-O(0.5)-UO2(OH) + 2 H<1+>	K02b
NE	Quartz	0.33	0			-7.78	»Si(w)-O(0.5)H + UO2<2+> + CO2 + H2O = »Si(w)-O(0.5)-UO2CO3(OH)<2-> + 3 H<1+>	K02b
NE	Quartz	0.33	0			-6.56	»Si(w)-O(0.5)H + UO2<2+> + H2O = »Si(w)-O(0.5)-UO2(OH) + 2 H<1+>	K02b
NE	Quartz	0.33	0			-5.57	»Si(s)-O(0.5)H + UO2<2+> + H2O = »Si(s)-O(0.5)-UO2(OH) + 2 H<1+>	K02b
NE	Quartz	0.33	0			-6.5	»Si(w)-O(0.5)H + UO2<2+> + CO2 + H2O = »Si(w)-O(0.5)-UO2CO3(OH)<2-> + 3 H<1+>	K02b
NE	Quartz	0.33	0			-5.28	»Si(w)-O(0.5)H + UO2<2+> + H2O = »Si(w)-O(0.5)-UO2(OH) + 2 H<1+>	K02b
TL	Quartz	0.32	0.00184		8.4	1.98	»Si(s)-OH + UO2<2+> = »Si(s)-O-UO2<1+> + H<1+>	FDZ06
TL	Quartz	0.32	0.00184		8.4	-1.88	»Si(s)-OH + UO2<2+> + H2O = »Si(s)-O-UO2(OH) + H<1+>	FDZ06

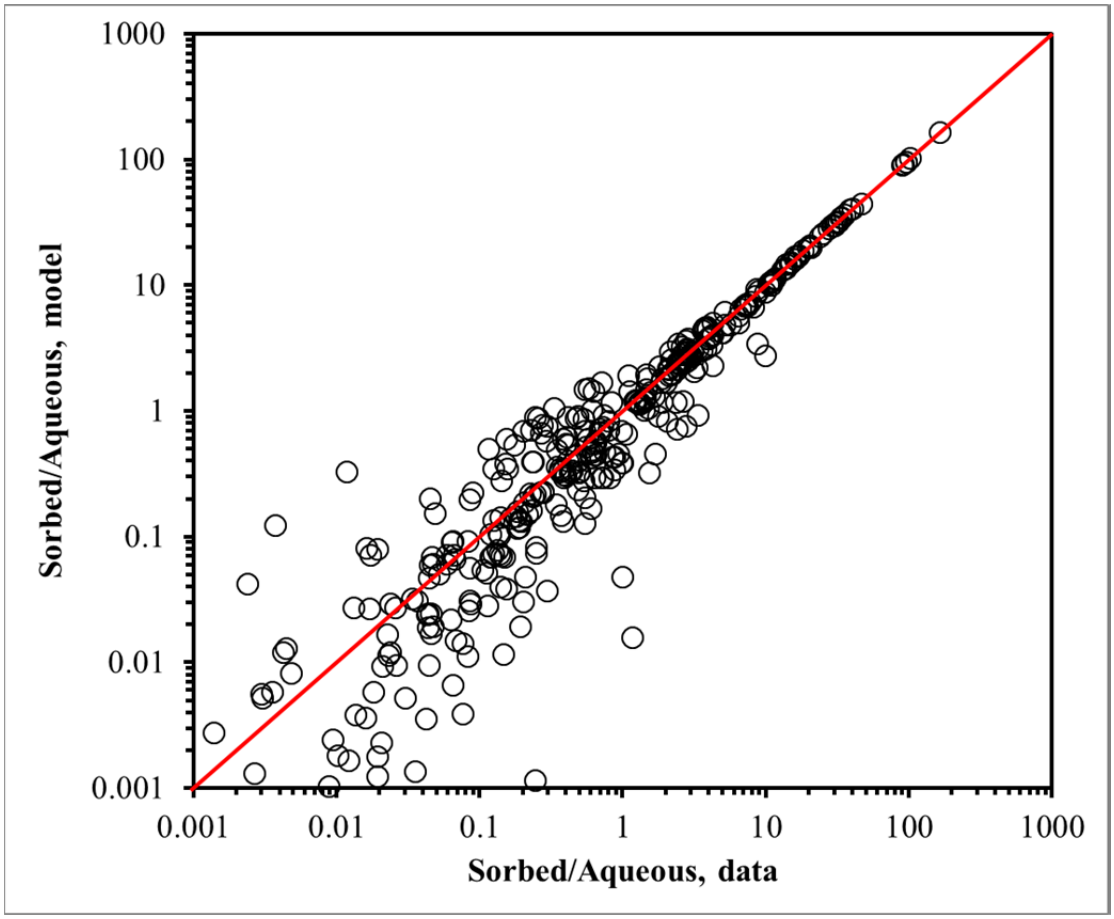

Figure 1. Comparison of data and model fits of the ratio of sorbed to aqueous concentrations for all batch sorption data contained in references identified by the RES^{3}T database for U(VI) sorption to quartz. Increasing scatter at low sorbed/aqueous ratios is a result of inherent uncertainties associated with samples with little to no U(VI) sorption. One-site non-electrostatic surface complexation model.

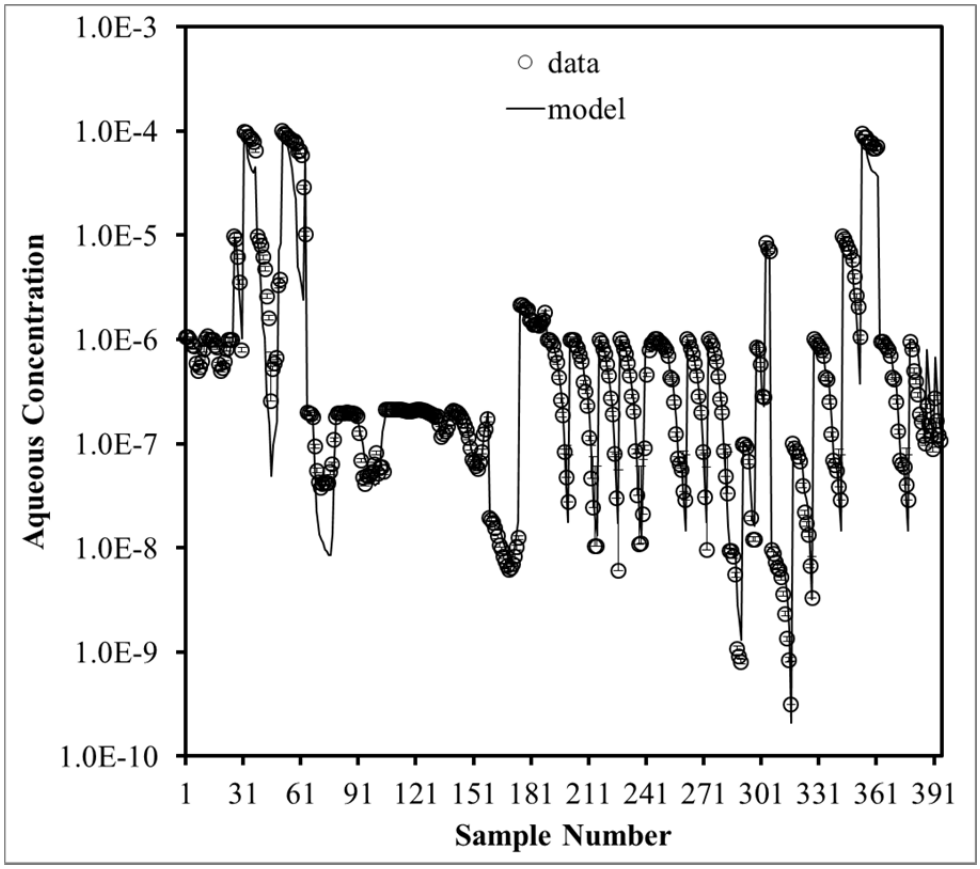

Figure 2. Comparison of measured and predicted U(VI) concentration in ~400 batch sorption data points digitized from the literature based on references contained in the RES^{3}T database for U(VI) sorption to quartz. One-site non-electrostatic surface complexation model.

4. Development of a Np(V) Ion Exchange Model

The aim of the ion exchange study was to isolate the ion exchange mechanism of Np(V) sorption to montmorillonite. Np(V) exchange on homoionic Na, K, Ca and Mg-montmorillonite was determined experimentally at pH 4.5 using Na^+, K^+, Ca^{2+} and Mg^{2+} as electrolyte cations at ionic strengths ranging from 0.001 to 0.1 M. This experimental data was then modeled to estimate selectivity coefficients for the exchange reactions. These coefficients are essential for accurate prediction of Np mobility in reactive transport models. The experimental work described herein was extracted from a manuscript recently published in Applied Geochemistry and attached to this document as Appendix B (Benedicto et al., 2014).

The experimental data obtained in this study indicate that Np ionic exchange depends on the major cation composition of the aqueous system, being especially limited by the presence of divalent cations such as Ca^{2+} and Mg^{2+} in solution. At basic conditions, ionic exchange becomes less significant and surface complexation of Np(V) will dominate. An ion exchange model was developed on the basis of the experimental data, which is consistent with selectivity coefficients

reported in the literature for the exchange between major cations and NpO_2^+ on montmorillonite. The recommended selectivity coefficients for Np(V) ionic exchange on montmorillonite, according to the Vanselow convention, are as follows: $\log\left({}^{NpO_2^+}_{Na^+}K_V\right) = -0.26$, $\log\left({}^{NpO_2^+}_{K^+}K_V\right) = -0.52$, $\log\left({}^{NpO_2^+}_{Ca^{2+}}K_V\right) = -0.69$, $\log\left({}^{NpO_2^+}_{Mg^{2+}}K_V\right) = -0.69$.

5. Planned FY14 Efforts

In FY15, we plan to continue our interaction with national and international partners in the development of thermodynamic models and databases. In particular, there is growing interest in expanding the capabilities of the RES^{3}T surface complexation development to capture raw sorption data and associated meta-data contained in published documents. A proof of principal effort will be used to test the robustness of data digitization software and optimal data storage and formatting structures that are compatible with the RES^{3}T database framework. One test case dataset (i.e. U(VI) binary sorption to silica) was digitized in FY13. More detailed evaluation of various surface complexation modeling approaches is planned for FY14.

6. Acknowledgments

This work was supported by the Used Fuel Disposition Campaign of the Department of Energy's Nuclear Energy Program. Prepared by LLNL under Contract DE-AC52-07NA27344.

7. References

Benedicto, A., Begg, J. D., Zhao, P., Kersting, A. B., Missana, T., and Zavarin, M., 2014. Effect of major cation water composition on the ion exchange on Np(V) on montmorillonite: NpO2+-Na+-K+-Ca2+-Mg2+ selectivity coefficients. Applied Geochemistry 47, 177-185.

Bradbury, M. H. and Baeyens, B., 1993. A general application of surface complexation modeling radionuclide sorption in natural systems. J. Colloid Interface Sci. 158, 364-371.

Bradbury, M. H. and Baeyens, B., 2009. Sorption modelling on illite. Part II: Actinide sorption and linear free energy relationships. Geochim. Cosmochim. Acta 73, 1004-1013.

Bradbury, M. H., Baeyens, B., and Thoenen, T., 2010. Sorption Data Bases for Generic Swiss Argillaceous Rock Systems. Nagra, Wettingen, Switzerland.

Davis, J., Ochs, M., Olin, M., Payne, T., and Tweed, C., 2005. Interpretation and prediction of radionuclide sorption onto substrates relevant for radioactive waste disposal using thermodynamic sorption models. OECD/Nuclear Energy Agency, Paris.

Dresden-Rossendorf, H.-Z., 2013. RES³T - Rossendorf Expert System for Surface and Sorption Thermodynamics. RES³T - Rossendorf Expert System for Surface and Sorption Thermodynamics, Dresden, Germany.

Geckeis, H., Lützenkirchen, J., Polly, R., Rabung, T., and Schmidt, M., 2013. Mineral–Water Interface Reactions of Actinides. Chemical Reviews 113, 1016-1062.

Helgeson, H. C., Delany, J. M., Nesbitt, H. W., and Bird, D. K., 1978. Summary and critique of the thermodynamic properties of rock-forming minerals. American Journal of Science 278, 1-229.

Holland, T. J. B. and Powell, R., 1985. An internally consistent thermodynamic dataset with uncertainties and correlations .2. Data and results. Journal of Metamorphic Geology 3, 343-370.

Holland, T. J. B. and Powell, R., 2011. An improved and extended internally consistent thermodynamic dataset for phases of petrological interest, involving a new equation of state for solids. Journal of Metamorphic Geology 29, 333-383.

Lemire, R. J., Berner, U., Musikas, C., Palmer, D. A., Taylor, P., and Tochiyama, O., 2013. Chemical Thermodynamics of Iron: Part I. OECD Nuclear Energy Agency, Issy-les-Moulineaux, France.

Ochs, M., Payne, T. E., and Brendler, V., 2012. Thermodynamic sorption modeling in support of radioactive waste disposal safety cases. A guideline document. OECD/NEA, Paris.

Powell, R. and Holland, T. J. B., 1985. An internally consistent thermodynamic dataset with uncertainties and correlations .1. Methods and a worked example. Journal of Metamorphic Geology 3, 327-342.

Robie, R. A. and Hemingway, B. S., 1995. Thermodynamic properties of minerals and related substances at 298.15K and 1 bar (105 pascals) pressure and at higher temperatures. U.S. Geological Survey, Reston, Virginia.

Wolery, T. J. and Sutton, M., 2013. Evaluation of Thermodynamic Data. Lawrence Livermore National Laboratory, Livermore, California.

8. Applendix A – Figures Digitized as part of the U(VI)-Quartz Surface Complexation Modeling Exercise

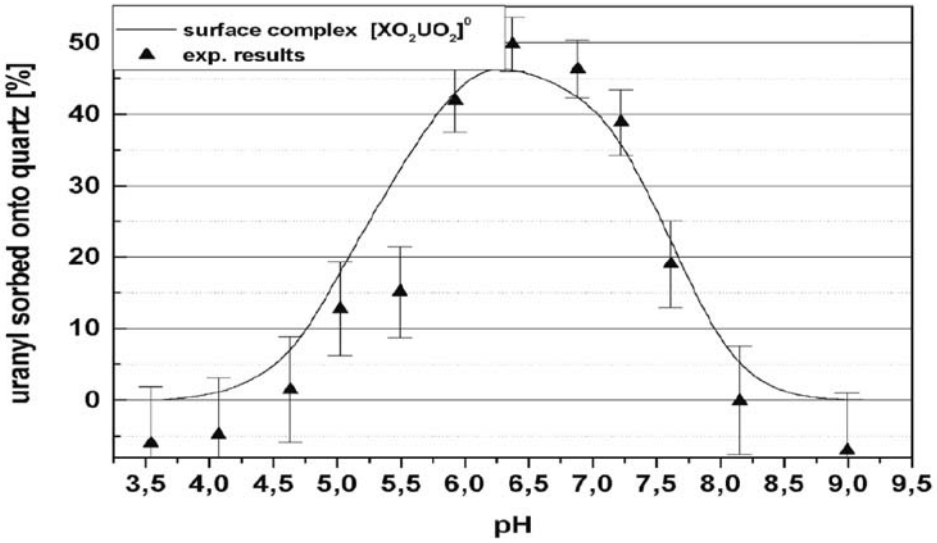

Figure A1. Sorption data from AZBN00a. See table 1 for details.

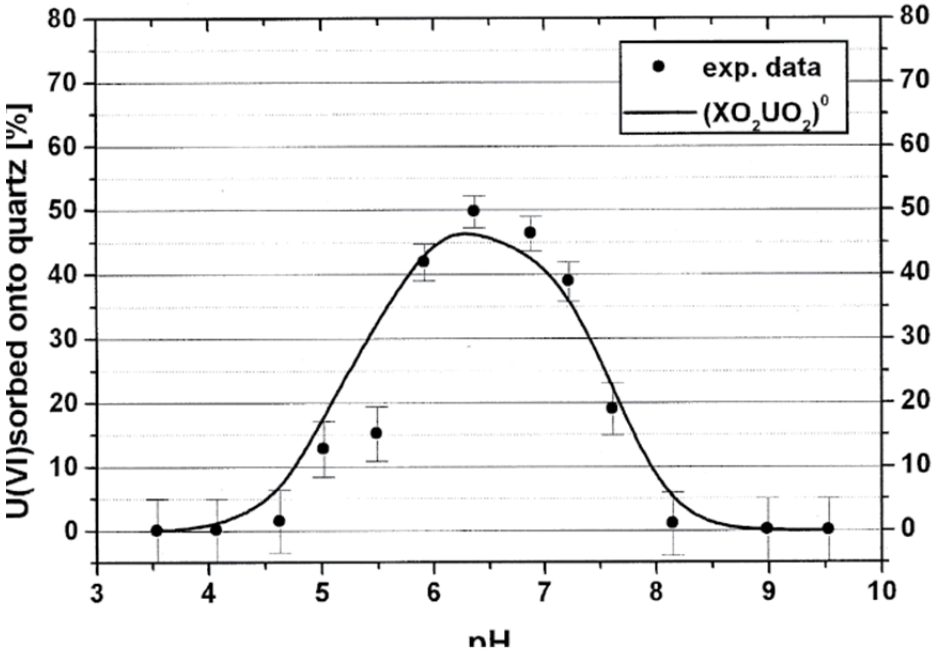

Figure A2. Sorption data from AZBN01. See table 1 for details.

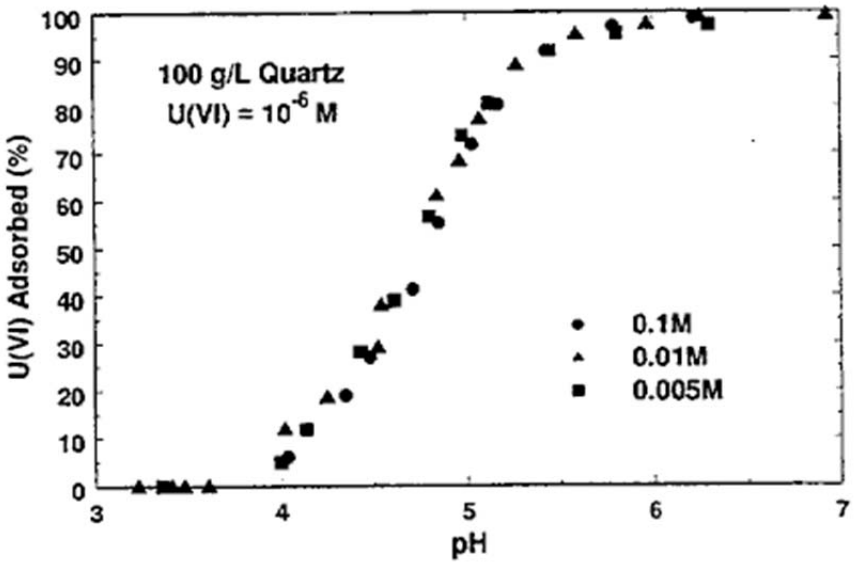

Figure A3. Sorption data from Figure 5-5 of DK01. See table 1 for details.

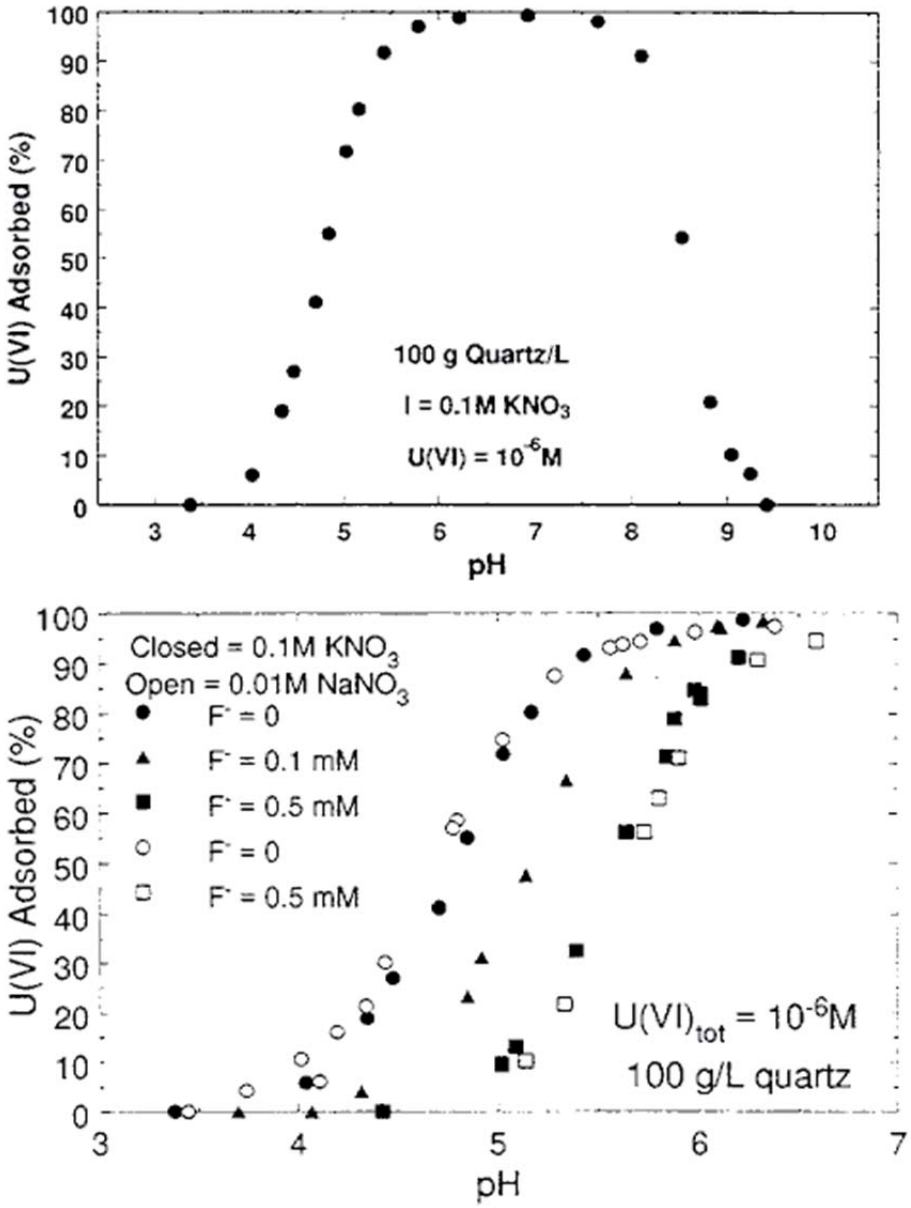

Figure A4. Sorption data from Figure 5-6 of DK01. See table 1 for details.

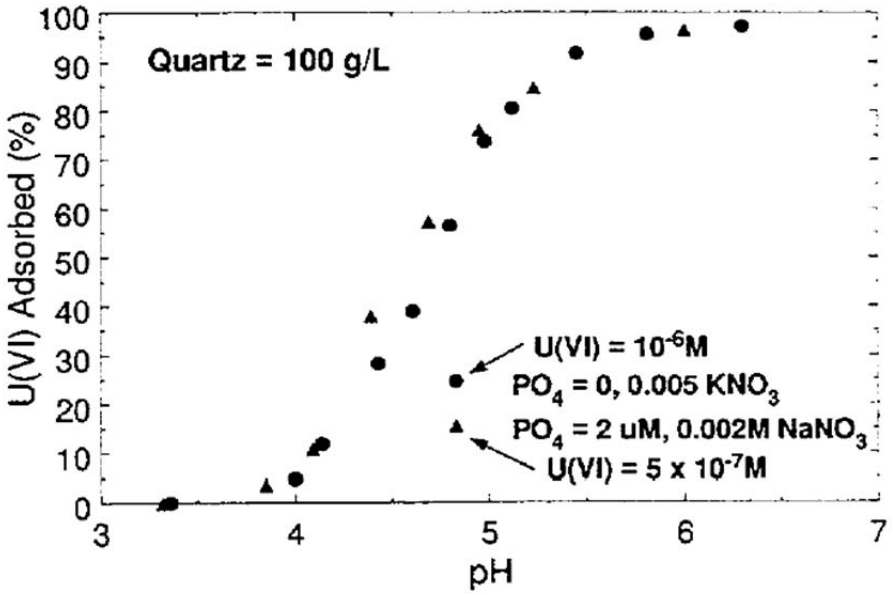

Figure A5. Sorption data from Figure 5-7 of DK01. See table 1 for details.

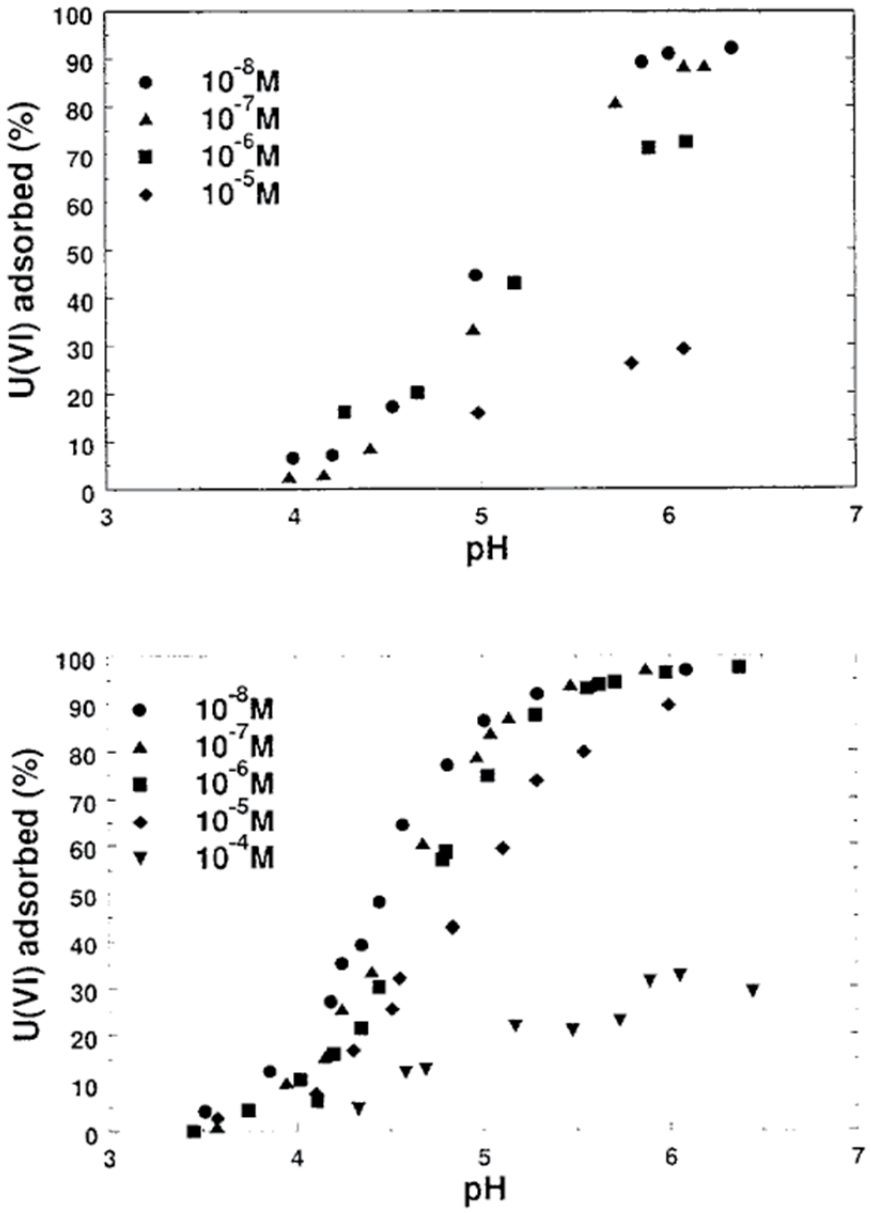

Figure A6. Sorption data from Figure 5-8 of DK01. See table 1 for details.

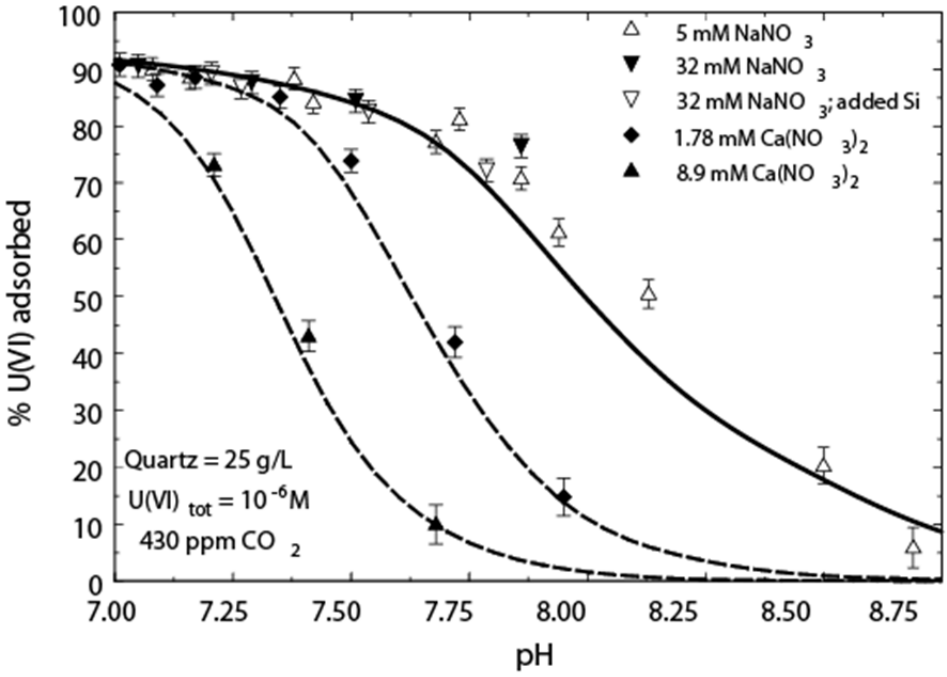

Figure A7. Sorption data from FDZ06. See Table 1 for details.

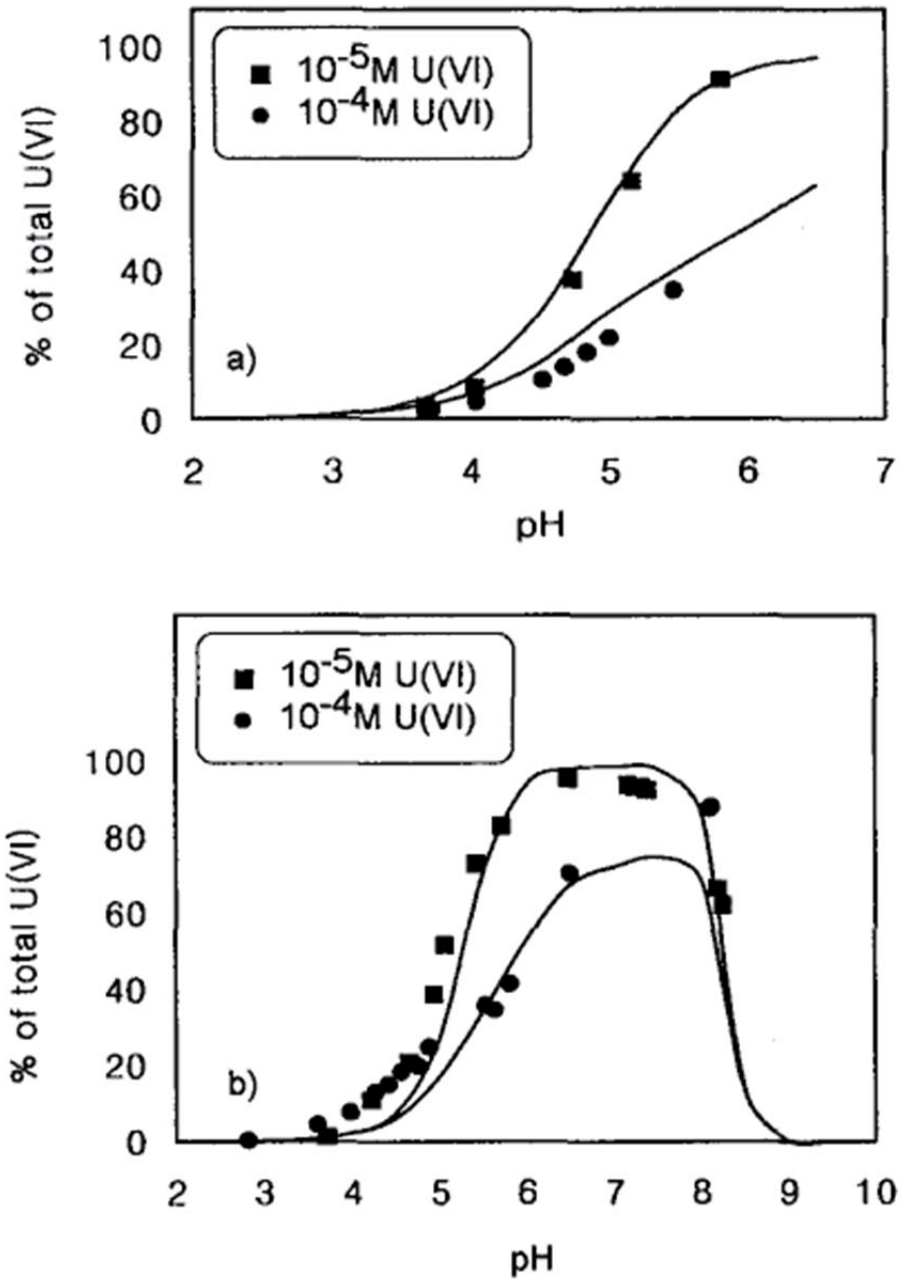

Figure A8. Sorption data from JHLCH99. See Table 1 for details.

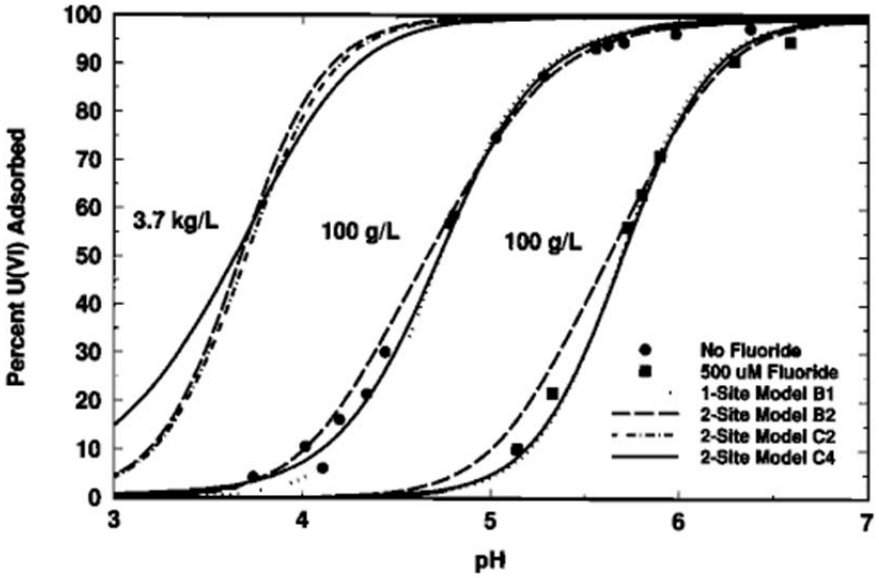

Figure A9. Sorption data from KCKD96. See Table 1 for details.

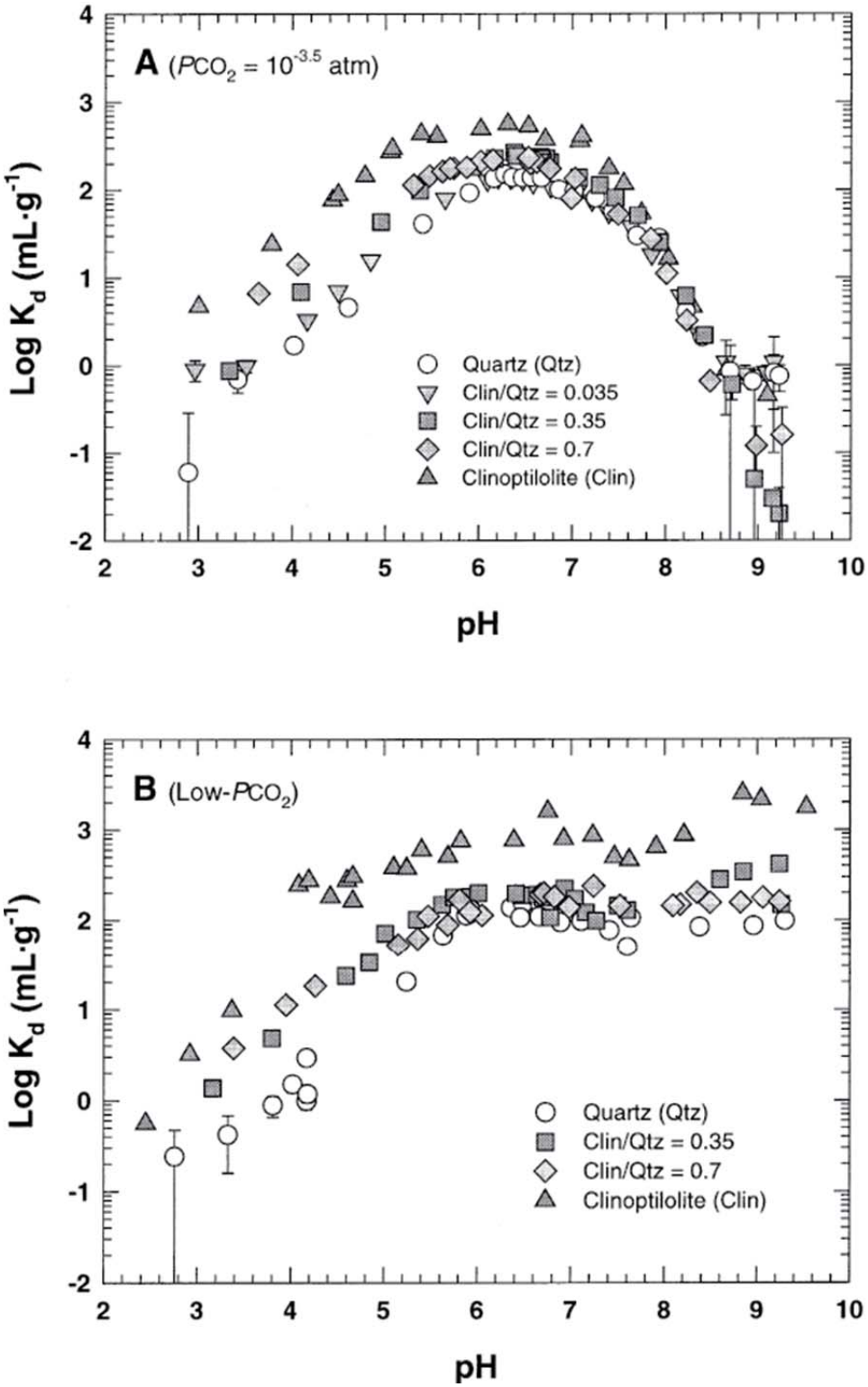

Figure A10. Sorption data from PJTP01. See Table 1 for details.

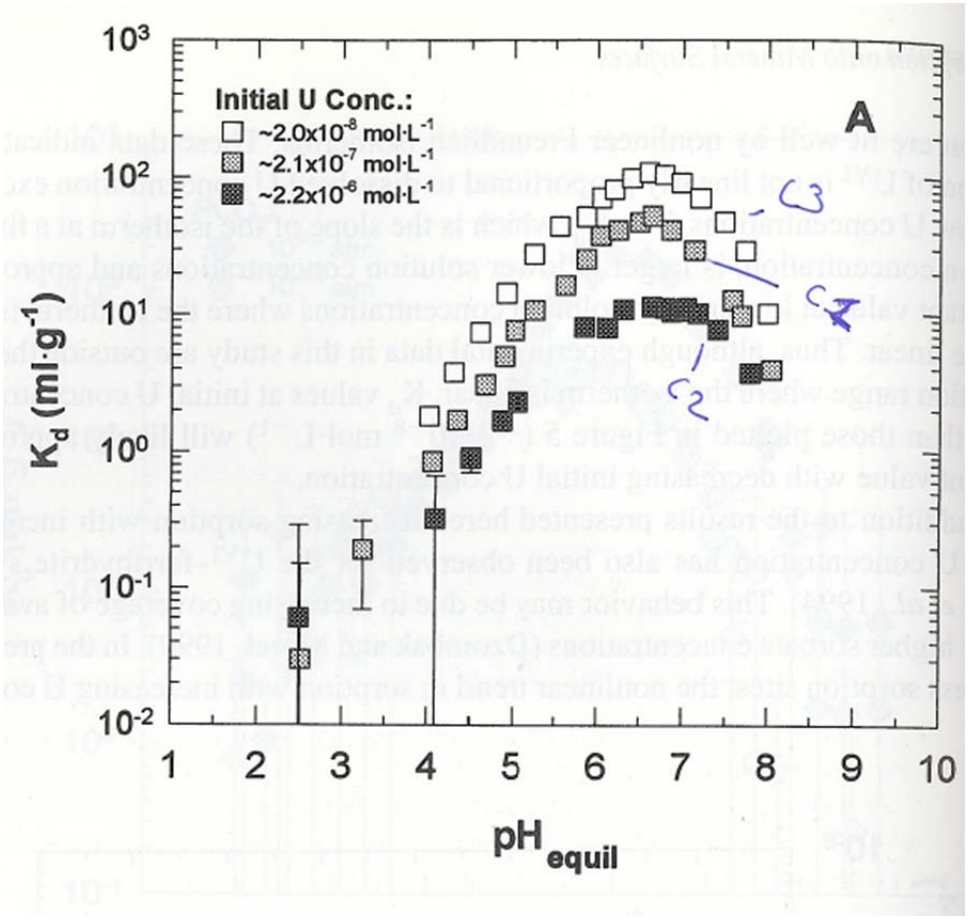

Figure A11. Sorption data from PTBP98 Figure 5. See Table 1 for details.

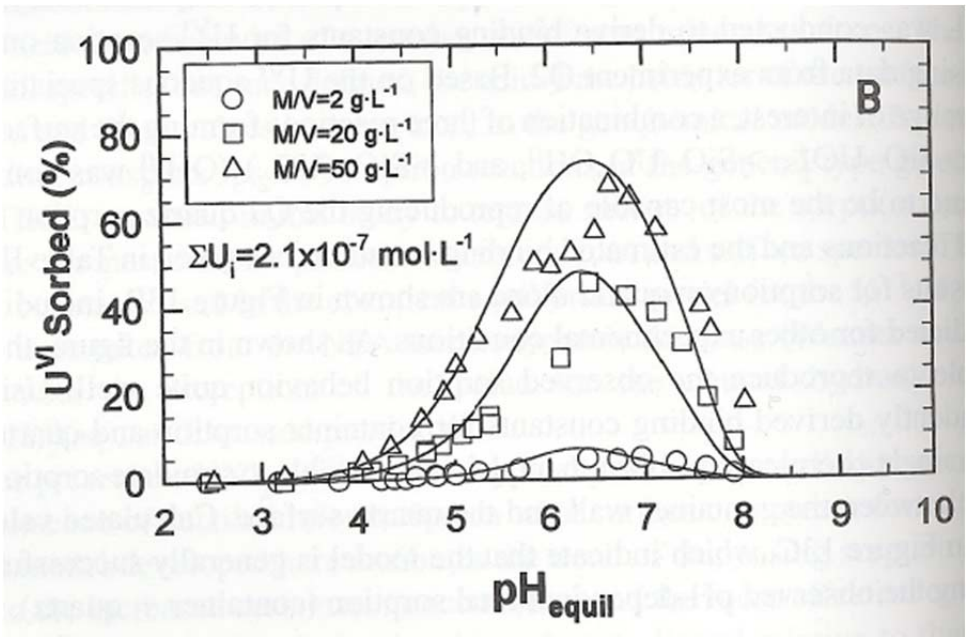

Figure A12. Sorption data from PTBP98 Figure 8. See Table 1 for details.

9. Applendix B – Manuscript Summarizing Np(V) Ion Exchange Data and Modeling Results

Applied Geochemistry 47 (2014) 177–185

Contents lists available at ScienceDirect

Applied Geochemistry

journal homepage: www.elsevier.com/locate/apgeochem

Effect of major cation water composition on the ion exchange of Np(V) on montmorillonite: NpO_2^+–Na^+–K^+–Ca^{2+}–Mg^{2+} selectivity coefficients

Ana Benedicto [a,b,*], James D. Begg [a], Pihong Zhao [a], Annie B. Kersting [a], Tiziana Missana [b], Mavrik Zavarin [a]

[a] Glenn T. Seaborg Institute, Physical & Life Sciences, Lawrence Livermore National Laboratory, 7000 East Avenue, Livermore, CA 94550, USA
[b] CIEMAT, Department of Environment, Avenida Complutense, 40, 28040 Madrid, Spain

ARTICLE INFO

Article history:
Available online 19 June 2014
Editorial handling by M. Kersten

ABSTRACT

Np(V) sorption was examined in pH 4.5 colloidal suspensions of nominally homoionic montmorillonite (Na-, K-, Ca- and Mg-montmorillonite). Ionic exchange on permanent charge sites was studied as a function of ionic strength (0.1, 0.01 and 0.001 M) and background electrolyte (NaCl, KCl, $CaCl_2$ and $MgCl_2$). An ion exchange model was developed using the FIT4FD program, which considered all experimental data simultaneously: Np sorption data, major cation composition of the electrolyte and associated uncertainties. The model was developed to be consistent with the ion exchange selectivity coefficients between the major cations reported in the literature and led to the following recommended selectivity coefficients for Np(V) ion exchange according to the Vanselow convention: $\log\left({}^{NpO_2^+}_{Na^+}K_V\right) = -0.20$, $\log\left({}^{NpO_2^+}_{K^+}K_V\right) = -0.46$, $\log\left({}^{NpO_2^+}_{Ca^{2+}}K_V\right) = -0.57$, $\log\left({}^{NpO_2^+}_{Mg^{2+}}K_V\right) = -0.57$. Both the experimental data and the estimated selectivity coefficients in this study are consistent with the limited Np(V) ion exchange and sorption data reported in the literature. The results indicate that, as expected, low ionic strengths favor Np(V) sorption when ion exchange is the main sorption mechanism (i.e. acidic to neutral pHs) and that the divalent cations Ca^{2+} and Mg^{2+} may be important in limiting Np(V) ionic exchange on montmorillonite.

1. Introduction

Neptunium (Np) is a transuranic element of particular environmental concern because its dominant isotope, ^{237}Np, has a long half-life (2.13×10^6 years) and high biological toxicity. In nuclear waste disposal scenarios and at long timescales, ^{237}Np will be one of several radiologically significant contributors (Kaszuba and Runde, 1999; Wescott et al., 1995; Wilson et al., 1994). In addition, ^{237}Np has been introduced into the environment as a consequence of the production and testing of nuclear weapons which has resulted in contamination at a number of locations including the Hanford Reservation and the Nevada National Security Site (formerly the Nevada Test Site) (Cantrell, 2009; Felmy et al., 2010; Smith et al., 2003).

The migration of actinides through the subsurface is highly influenced by their interaction with minerals and rocks. Clay minerals, such as montmorillonite, are ubiquitous in the environment and given their surface properties, sorption capacity and colloidal behavior, they will likely play an important role in actinide retention-transport processes. Furthermore, montmorillonite is a major component of proposed barriers for the geological nuclear waste repository designs of many countries, for example, Germany, France and Switzerland (Hoth et al., 2007; Nagra, 2002; OECD, 2006). Montmorillonite is a 2:1 clay mineral and consists of two SiO_4 tetrahedral (T) sheets bound to either side of an AlO_6 octahedral (O) sheet (expressed as T:O:T) (Dixon, 1989). Isomorphic substitutions of Al and Si give a permanent negative charge to the structure that is compensated by exchange cations. The electrostatic attraction between the charged layers and the exchangeable cations causes the cohesion of the T:O:T layers. As a result, the total cation exchange capacity is distributed between the inner surfaces in the interlayer spacing and the outer surfaces of the clay particles. In addition, montmorillonite exhibits pH-dependent charge in the broken silanol and aluminol edges of the T:O:T sheets. Therefore, two mechanisms of sorption exist on montmorillonite: cation exchange, which can occur at permanent charge sites as well as on the variably charged silanol and aluminol groups, and surface complexation which occurs on the variably charged silanol and aluminol groups in the sheet edges and is pH dependent (Bradbury and Baeyens, 1997).

The sorption of Np is controlled by both its redox and aqueous speciation (Bondietti and Francis, 1979; Kaszuba and Runde, 1999;

* Corresponding author. Present address: CEA, Centre d'études de Saclay, L3MR, 91191 Gif-sur-Yvette, France. Tel.: +34 636157022.
E-mail address: ana-benedicto@hotmail.com (A. Benedicto).

http://dx.doi.org/10.1016/j.apgeochem.2014.06.003
0883-2927/

Law et al., 2010; Runde et al., 2002). Under a wide range of oxic conditions, the pentavalent oxidation state, in the form of NpO_2^+, will dominate (Choppin, 2006; Kaszuba and Runde, 1999). NpO_2^+ has a relatively low sorption affinity for most minerals and rocks (Triay et al., 1993), resulting in its high aqueous mobility. Although Np(IV) may exist under certain environmental conditions, the higher predicted mobility of Np(V) makes it the preferred form for studying transport scenarios. Given its long half-life, its predicted high mobility, and the importance of clays both in the geosphere and nuclear repository scenarios, understanding Np(V) sorption to clays such as montmorillonite is of particular interest. Moreover, knowledge of the sorption behavior of Np(V) may provide insight into the sorption behavior of other pentavalent actinides such as Pu(V) that are more redox sensitive and experimentally more difficult to study (Turner et al., 1998; Zavarin et al., 2012).

Under aerobic conditions and at circumneutral pH values, Np(V) sorption to montmorillonite is likely to be dominated by surface complexation at the variably charged sorption sites (Bradbury and Baeyens, 2006; Turner et al., 1998). However, at pH values below pH 6, cation exchange on permanent charge sites is expected to be the dominant sorption mechanism (Bradbury and Baeyens, 2006; Kozai et al., 1996; Nagasaki and Tanaka, 2000; Sabodina et al., 2006; Sakamoto et al., 1990; Turner et al., 1998; Zavarin et al., 2012). Sorption by ion exchange on permanent charge sites is dependent on the composition of the clay exchange sites (Jensen, 1973), commonly occupied by Na^+, K^+, Mg^{2+} and Ca^{2+}, which is, in turn, strongly dependent on the aqueous conditions and electrolyte composition. However, most of the studies in the literature have so far focused on Np(V)–Na^+ ion exchange. Conversely, exchange with other common cations such as Ca^{2+}, Mg^{2+} or K^+ is not well known despite being fundamental to understanding Np(V) sorption in natural systems. Kozai et al. (1996) investigated Np(V) exchange with a range of cations (Na^+, Mg^{2+}, Cs^+, Ca^{2+}, K^+ and Li^+). However the effect of the electrolyte composition and its concentration was not studied (all experiments were performed in 0.1 M $NaClO_4$), which limits attempts to estimate ion exchange selectivity coefficients. Mironenko et al. (2006) investigated Np(V) exchange with Mg^{2+} and Ca^{2+} at pH around 6.5, where sorption by surface complexation cannot be excluded.

The aim of this study was to isolate the ion exchange mechanism of Np(V) sorption on to the permanent charge sites of montmorillonite and to estimate the selectivity coefficients of Np(V) with the main ions expected to be present in typical groundwaters. Np(V) exchange on homoionic Na, K, Ca and Mg-montmorillonite was determined experimentally at pH 4.5 using Na^+, K^+, Ca^{2+} and Mg^{2+} as electrolyte cations at ionic strengths ranging from 0.001 to 0.1 M. This experimental data was then modeled to estimate selectivity coefficients for the exchange reactions. These coefficients are essential for accurate prediction of Np mobility in reactive transport models. Finally we applied our calculated values to various natural water scenarios in order to illustrate the importance of permanent charge site cation exchange under different environmental conditions.

2. Materials and methods

2.1. Montmorillonite suspensions preparation

Unless stated otherwise, all solutions were prepared using ultrapure water (Milli-Q Gradient System, >18 MΩ cm) and ACS grade chemicals without further purification. The montmorillonite used in the experiments was SWy-2 montmorillonite (Source Clays Repository of the Clay Minerals Society, *CMS*). It was pre-conditioned and purified using the procedure reported in Zavarin et al. (2012). Briefly, the montmorillonite was (1) pre-treated in a 0.001 M HCl solution to dissolve any soluble salts, (2) reacted with a H_2O_2 solution to minimize the reducing capacity of any impurities, (3) treated in a 0.1 M NaCl solution to produce a homoionic clay suspension, (4) dialyzed in Milli-Q water to remove excess salts, and (5) centrifuged at 180*g* for 5 min and then 2500*g* for 6 h to isolate particles in the size range >2 μm and <50 nm for use in the experiments. The clay was then dried at 40 °C.

A small portion of the dried clay was lightly ground then used for a surface area measurement (N_2(g)-BET Quadrasorb SI). The particles had a surface area of 31.5 $m^2\ g^{-1}$ which is consistent with the reported value of 31.8 $m^2\ g^{-1}$ (reported by the *CMS*). XRD patterns were obtained on a Bruker D8 X-ray diffractometer and compared favorably with the montmorillonite reference pattern from the International Centre for Diffraction Data. No additional mineral phases were observed indicating that the prepared montmorillonite was relatively pure. The *CMS* reported a cation exchange capacity of 764 meq kg^{-1} for the SWy-2 clay for the <2 μm size fraction.

Stock suspensions of the K, Ca or Mg exchanged montmorillonite were prepared by dialyzing 5 g of pre-conditioned Na-montmorillonite in 500 mL of 0.1 M KCl, $CaCl_2$ or $MgCl_2$, respectively (Kozai et al., 1996). The electrolyte was changed every day for one week. Following homoionization, the clays were washed repeatedly with Milli-Q water to remove excess salts. For the sorption experiments, suspensions of 2 g L^{-1} were prepared by diluting homoionized clays in the appropriate electrolyte at ionic strengths of 0.1, 0.01 and 0.001 M.

2.2. Np(V) solution

The isotope ^{237}Np was used in all batch sorption experiments. Separation of ^{237}Np from ^{233}Pa was performed using the procedure of Pickett et al. (1994). The Np oxidation state was manipulated by heating in concentrated HNO_3. The oxidation state of Np in the purified solution was checked using a Cary 500 UV–Vis spectrophotometer. Observation of a single absorption band at 979 nm verified the presence of Np(V) (Waggener, 1958). For sorption experiments, ^{237}Np stock solutions of 5×10^{-4}, 5×10^{-5}, and 5×10^{-6} M were prepared.

2.3. Sorption batch experiments

Np sorption isotherms were performed using the Na, K, Ca, and Mg-montmorillonite suspensions (2 g L^{-1}) and spiking them with ^{237}Np to achieve concentrations between 2×10^{-8} and 5×10^{-6} M. Experiments were carried out in polyethylene tubes containing homoionic montmorillonite suspensions at three ionic strengths: 0.1, 0.01 and 0.001 M. The pH was fixed to 4.5 in order to isolate permanent charge site cation exchange as the unique Np(V) sorption mechanism (Zavarin et al., 2012). The pH of each experiment was checked with an Orion 920A pH meter and electrode calibrated with three standard buffer solutions. Given the acidity associated with the Np stock following purification, the pH was readjusted to 4.5 with 0.1 M NaOH as necessary following spiking. After spiking, the tubes were sealed and placed on an orbital shaker at room temperature for 6 days in order to achieve sorption equilibrium (Zavarin et al., 2012). The pH of the experiments was checked at the final sampling point and a value of 4.4 ± 0.2 was found in all the samples. Due to the acidic nature of the Np(V) spike and the need to adjust solution pH to 4.5, solution ionic strengths increased upon addition of Np(V). However, cation concentrations were monitored, as described below, so as to account for any changes in solution composition.

The ^{237}Np concentration was analyzed using a Perkin Elmer Liquid Scintillation Analyzer (LSA) model Tri-Carb 2900TR in alpha–beta discrimination mode. After the sorption period, total

Np activity in the suspension ($[Np]_{tot}$) was measured. The difference between added Np and the Np in suspension was up to 13%, indicating some Np sorption to tube walls. However, normalizing all calculations to the total Np activity in suspension ($[Np]_{tot}$) avoided any artifacts associated with Np(V) loss to container walls in our sorption distribution coefficient calculations. Samples were then centrifuged at 7600*g* for 2 h to achieve a <30 nm particle size cut-off. Np activity in the supernatant ($[Np]_{sol}$) was then determined. Na^+, K^+, Ca^{2+} and Mg^{2+} concentrations in the supernatant were determined by ion chromatography (IC) using a Dionex-ICS 600.

The sorption distribution coefficient, K_d (mL g^{-1}), was calculated by means of the following equation:

$$K_d = \frac{[Np]_{tot} - [Np]_{sol}}{[Np]_{sol}} \frac{1}{[mont]} \quad (1)$$

where [mont] is the montmorillonite concentration in the suspension (g mL^{-1}).

2.4. Np(V) speciation and sorption modeling

In this study, Np(V) speciation, Np sorption data fitting, and ion exchange simulations were carried out using the FIT4FD code (Zavarin et al., 2005). The FIT4FD modeling of sorption data and determination of Np ion exchange selectivity coefficients was conducted by fitting all sorption isotherms simultaneously. The FIT4FD code allowed us to account for the unique cation composition of each sample and the associated measurement uncertainties (see Supporting Information). The simultaneous fitting of all ion exchange data ensured that the resulting ion exchange constants (and their associated uncertainties) were self-consistent across the entire range of solution compositions examined. Ion exchange selectivity coefficients were determined using both the Vanselow and Gaines–Thomas conventions as described in detail in the following section.

The NEA thermodynamic database used for aqueous speciation included the hydrolysis and carbonate complexation constants selected by Lemire et al. (2001) and Neck et al. (1994) (see Supporting Information). Activity correction was based on the Davies equation.

The ion exchange reaction between a cation, *B*, with charge z_B, in the aqueous phase and a cation, *A*, with charge z_A, at the cation exchange site of a clay can be represented by:

$$z_B Clay(A) + z_A B^{z_B+} \leftrightarrow z_A Clay(B) + z_B A^{z_A+} \quad (2)$$

The cation exchange reaction can be described in terms of selectivity coefficients which indicate the sorption preference between two ions of different charge and size for the exchange site. An example of a calculation of the selectivity coefficient for an *A*/*B* exchange is shown in Eq. (3). It should be noted that the selectivity coefficient is not necessarily a true thermodynamic exchange constant, since it has been shown, in some cases, to vary with factors such as the exchanger composition or the clay tactoid size (Jensen, 1973; Tournassat et al., 2011).

In the literature, various conventions are used to define selectivity coefficients. The Gaines–Thomas and the Vanselow conventions are commonly used in different speciation codes and by different authors (e.g. Gaines–Thomas convention: Bethke and Yeakel, 2009; Bolt, 1982; Bradbury and Baeyens, 2000, 2009; Maes and Cremers, 1977; Missana and García-Gutiérrez, 2007; Parkhurst and Appelo, 1999; Poinssot et al., 1999; Tournassat et al., 2007; Yariv and Cross, 1979; e.g. Vanselow convention: Bethke and Yeakel, 2009; Fletcher and Sposito, 1989; Parkhurst and Appelo, 1999; Schindler et al., 1987; Shaviv and Mattigod, 1985; Tournassat et al., 2007; Zavarin et al., 2005). In the case of homovalent ion exchange where $z_A = z_B$, both conventions lead to equivalent selectivity coefficients. However, in the case of heterovalent ion exchange, the two conventions are not equivalent.

Following the Gaines–Thomas convention (Gaines and Thomas, 1953), the selectivity coefficient (K_{GT}) is expressed by:

$${}^{B}_{A}K_{GT} = \frac{(E_B)^{z_A}(a_A)^{z_B}}{(E_A)^{z_B}(a_B)^{z_A}} \quad (3)$$

where a_A and a_B are the activities of the cations *A* and *B* respectively, and E_A and E_B are the equivalent fractional occupancies. The equivalent fractional occupancy is defined as the equivalents of sorbed cation per unit mass of clay (eq g^{-1}) divided by the cation exchange capacity CEC (eq g^{-1}).

In the Vanselow convention (Mcbride, 1994; Sposito, 1981), the selectivity coefficient (K_V) for the reaction is defined as follows:

$${}^{B}_{A}K_{V} = \frac{(M_B)^{z_A}(a_A)^{z_B}}{(M_A)^{z_B}(a_B)^{z_A}} \quad (4)$$

where M_A and M_B represent the mole fraction of the ion in the exchange phase. The mole fractional occupancy is defined as the moles of sorbed cation per mass (mol g^{-1}) divided by total moles in the clay exchange complex (mol g^{-1}).

3. Results and discussion

3.1. Np(V) aqueous speciation

The ion exchange of Np(V) will be dependent on its speciation in solution. Fig. 1 shows Np(V) aqueous speciation as a function of pH at ionic strength 0.1 M in the presence of monovalent cations (NaCl or KCl) and divalent cations ($CaCl_2$ or $MgCl_2$), for a Np(V) concentration of 5.5×10^{-6} M (Np speciation did not change across the range of Np concentrations used in this work (2.0×10^{-8} – 5.5×10^{-6} M), data not shown).

NpO_2^+ is predicted to be the dominant aqueous species (>94.5%) at the pH value (4.5) used in these experiments. However we note that at pH 4.5 the uncharged species NpO_2Cl^0 will also be present, albeit as a minor component (<5.5%). For the same ionic strength, the percentage of NpO_2Cl^0 is slightly lower in the presence of divalent cation (Ca and Mg) electrolytes, due to the lower Cl^-

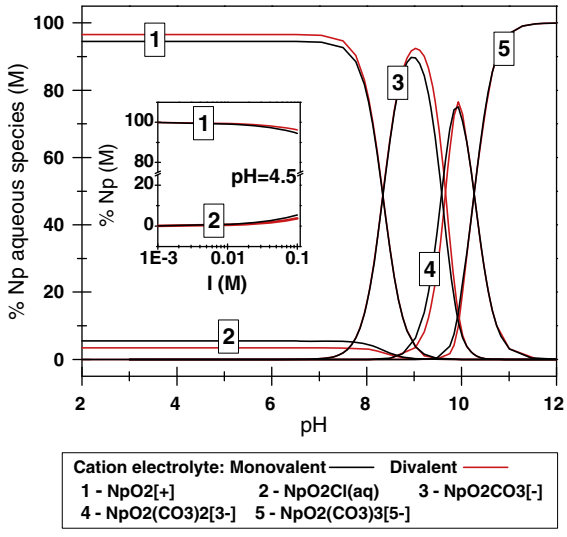

Fig. 1. Np(V) aqueous speciation as a function of pH in equilibrium with atmospheric CO_2 ($p_{CO2} = 10^{-3.4}$ atm) in electrolyte ($I = 0.1$ M) composed of monovalent cations (NaCl or KCl) or divalent cations ($CaCl_2$ or $MgCl_2$). Inset shows change in Np(V) aqueous speciation as a function of ionic strength (pH = 4.5).

concentration. The inset in Fig. 1 illustrates Np(V) aqueous speciation as a function of ionic strength at pH 4.5. The percentage of Np as NpO_2^+ decreases slightly in favor of NpO_2Cl^0 as ionic strength increases, but the percentage change (from 0% to 5.5%) is relatively minor. Thus, the presence of NpO_2Cl^0 will not significantly affect the ion exchange behavior of Np(V) over the range of solution compositions investigated.

3.2. Cation composition of batch sorption samples

Interpretation of Np ion exchange data requires consideration of the concentration of all cations in solution at equilibrium. This is important as the composition of the electrolyte varied due to adjustments in pH made to counter the acidity of the Np(V) spike addition and because the clay likely released trace amounts of other cations or impurities not removed during the homoionization process (Baeyens and Bradbury, 2004; Poinssot et al., 1999). For example, it is possible that Al^{3+} will also be present in solution due to dissolution of the mineral and this may affect exchange constants at low ionic strength. Although not measured directly, previous work indicates that Al^{3+} concentrations are likely to be less than 10^{-6} M (Benedicto et al., 2014). Al^{3+} species were not considered in our modeling approach.

Fig. 2 shows the concentrations of Na^+, K^+, Ca^{2+} and Mg^{2+} measured in solution at the end of each experiment as a function of the final Np concentration in solution. Significant levels of Na^+ are present in each sample in addition to the principal cation, as expected. The Na^+ concentration in solution increases with Np concentration and follows the same trend for all four sets of "homoionic" ion exchange systems. The significant concentration of Na^+ and trace amounts of other cations found in all solutions will likely impact the ion exchange behavior of Np(V) on montmorillonite. This effect was indeed observed in the Np(V) sorption data and is described in the following section. Accordingly, it was necessary to account for the actual fluid ion composition of each experiment when determining Np(V) selectivity coefficients. An increase in Ca^{2+} and Mg^{2+} concentration with increased Np_{sol} concentration was observed at the lowest ionic strength for the Na-montmorillonite experiments. We cannot speculate further as to why such an increase is observed but again we note that the actual measured cation concentrations for each experiment were used in our modeling effort.

3.3. Np(V) sorption data

Np(V) sorption to homoionic montmorillonite (Na, K, Mg or Ca) suspended in corresponding electrolyte solutions (NaCl, KCl, $MgCl_2$ or $CaCl_2$, respectively) at three initial ionic strengths (0.1, 0.01 and 0.001 M) was measured over a range of initial Np concentrations ($2.0 \times 10^{-8} - 5.5 \times 10^{-6}$ M). The Np distribution coefficients (K_d) as a function of the Np concentration in solution for each batch system (Na-, K-, Ca- and Mg-montmorillonite) are plotted in Fig. 3. It is important to note that Na^+ concentration also changes as a function of Np concentration, as discussed previously.

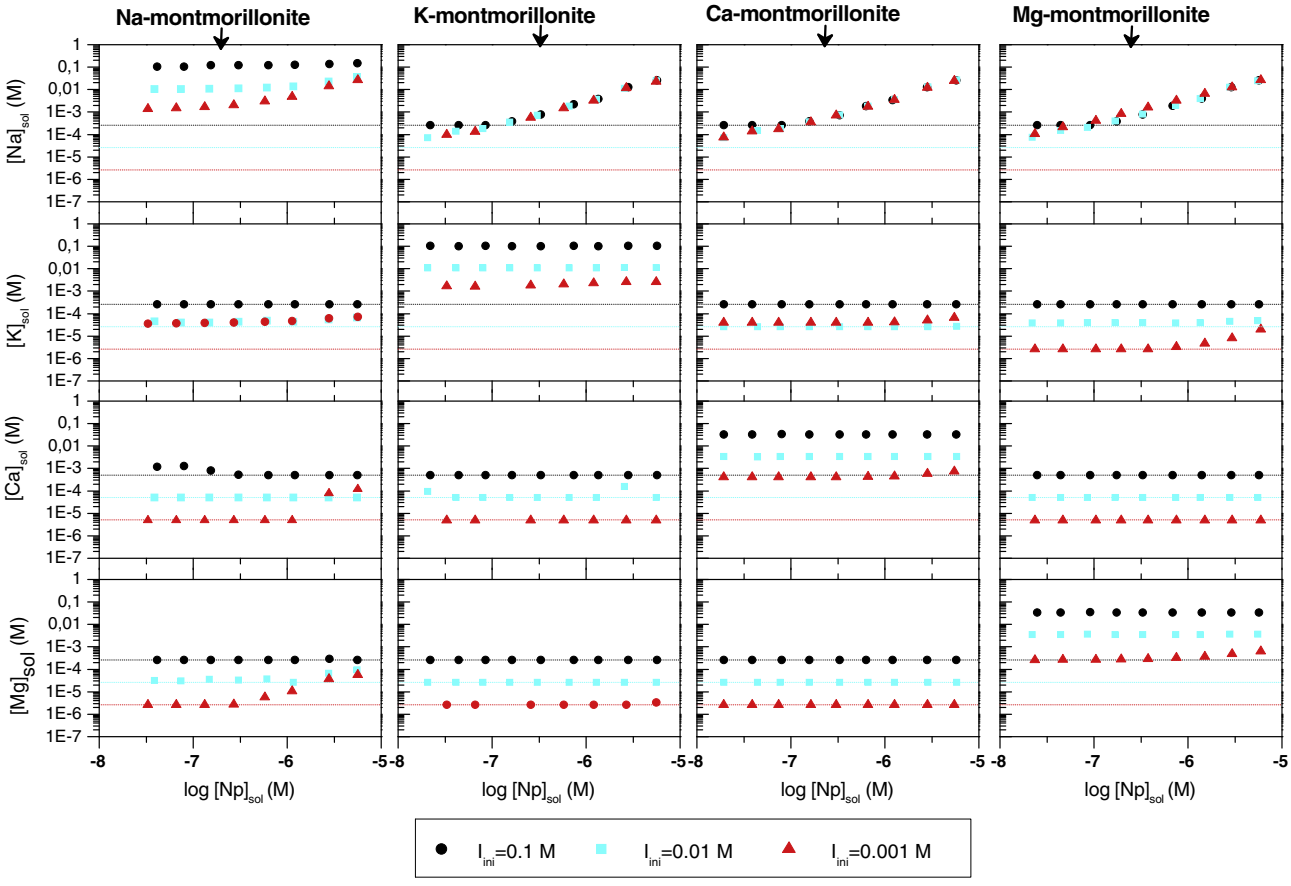

Fig. 2. Cation concentration of the electrolyte at the end of the experiment vs. final Np concentration in solution (Np_{sol}), at pH 4.5 and initial ionic strengths of 0.1 M, 0.01 M and 0.001 M in each system studied (Na, K, Ca and Mg-montmorillonite). The dashed lines represent estimated cation quantification limits at each ionic strength. Variation in specific cation quantification limits as a function of ionic strength are an artifact of the necessary dilution of samples imposed by total cation concentration for sample analysis. Estimated error on cation concentration is 5% and is not shown on this plot.

Fig. 3 shows a clear difference in sorption behavior between Np(V) sorption in monovalent Na^+/K^+ solutions (Fig. 3a and b) and divalent Ca^{2+}/Mg^{2+} solutions (Fig. 3c and d). Kozai et al. (1996) also reported lower Np(V) sorption on homoionic Ca- and Mg-montmorillonite relative to K- and Na-montmorillonite.

At low ionic strength (0.001 M) and at low Np concentrations, the K_d values in Na-montmorillonite and K-montmorillonite are between 130 and 210 mL g^{-1}. Comparison of these values with other data from the literature is not straightforward given the complex composition of the final electrolyte, as shown in Fig. 2. Nevertheless, to a first approximation, these K_d values are higher than the K_d of 24 ± 5 mL g^{-1} reported by Zavarin et al. (2012) for montmorillonite in 0.01 M NaCl (pH 3 to 5) and much higher than the K_d of 4–6 mL g^{-1} reported by Turner et al. (1998) for montmorillonite in 0.1 M $NaNO_3$ (pH < 5.5). Thus, this study in addition to the work of Zavarin et al. (2012) and Turner et al. (1998) illustrates a consistent pattern of ionic strength dependence of Np(V) sorption at low pH and provides strong evidence that sorption at low pH is dominated by ion exchange processes on permanent charge sites.

As the Np concentration increases, the K_d values decrease significantly for monovalent cation systems (Fig. 3a and b). Careful examination of the background electrolyte composition (Fig. 2) indicates that the ionic strength of the solutions increases with Np(V) concentration due to the Np spike acidity compensation. Thus, the apparent decrease in Np(V) ion exchange at higher Np(V) concentrations may be more correctly attributed to changes in ionic strength, as we will demonstrate in the following modeling effort.

In monovalent exchange experiments, increasing the ionic strength decreases K_d values, with minimal sorption seen at the highest ionic strength (Fig. 3). The observation of low sorption at high ionic strength is consistent with Zavarin et al. (2012) who reported a K_d of <6 mL g^{-1} in 1 M NaCl solutions. Further, such ionic strength dependence is consistent with the ion exchange mechanisms detailed in reactions (3) and (4) which imply that the extent of sorption of a cation will be dependent on the activity of the competing cation (Langmuir, 1997).

A decrease in Np(V) sorption with increasing ionic strength is not apparent in the divalent cation exchange experiments (Fig. 3c and d). This is both due to the low K_d values (with corresponding large associated uncertainties) and to the fact that changes in the divalent cation concentration have less influence on absolute K_d values than changes in the monovalent cation concentration. Such behavior is consistent with the ionic exchange mechanism. In the ion exchange processes represented in Eq. (2), the theoretical dependence on ionic strength can be derived from Eqs. (1) and (3). When the cation adsorbate B is present at trace level, the dependence can be expressed as follows (Bradbury and Baeyens, 1995):

$$z_A \log(K_d) = -z_B \log[A] + \log\left(\frac{{}^{B}_{A}K_{GT}(CEC)^{z_A}\gamma_B^{z_A}}{z_B^{z_A}\gamma_A^{z_B}}\right) \quad (5)$$

where $[A]$ is the concentration of the cation A in solution (M) and γ_A and γ_B are the solution activity coefficients of cations A and B.

Thus, for homovalent exchange (NpO_2^+–Na^+ or NpO_2^+–K^+) the dependence of the logarithm of the distribution coefficients ($\log(K_d)$) with the logarithm of the concentration of the main ion of the electrolyte $\log[A]$ is represented by a line with a slope of −1. For NpO_2^+–Ca^{2+} or NpO_2^+–Mg^{2+} exchange, this dependence is a line with slope −0.5.

Given the higher Np sorption observed in the presence of monovalent cations compared to divalent cations, we expect that ${}^{NpO_2^+}_{Na^+}K$ and ${}^{NpO_2^+}_{K^+}K$ selectivity coefficients to be significantly greater than ${}^{NpO_2^+}_{Ca^{2+}}K$ and ${}^{NpO_2^+}_{Mg^{2+}}K$ selectivity coefficients, as will be demonstrated in the modeling efforts below.

3.4. Modeling Np(V) ion exchange on montmorillonite

For simple binary ion exchange experiments, the selectivity coefficient between two cations can be determined by fitting experimental data to equations 3 or 4. In our study, this approach is not possible because solution conditions vary both in ionic strength and in electrolyte cation composition (Fig. 2). As a result, selectivity coefficients between cation pairs (e.g. ${}^{NpO_2^+}_{Na^+}K$, ${}^{NpO_2^+}_{K^+}K$, ${}^{NpO_2^+}_{Ca^{2+}}K$ and ${}^{NpO_2^+}_{Mg^{2+}}K$ cannot be fitted individually. The FIT4FD code allows for the fitting of all batch isotherm data simultaneously and can account for the measured cation composition (i.e. Na, K, Ca, Mg, and Np) of each individual sample in the fitting process. In addition, uncertainties for each measured cation concentration can be accounted for in the minimization routine (see Supporting

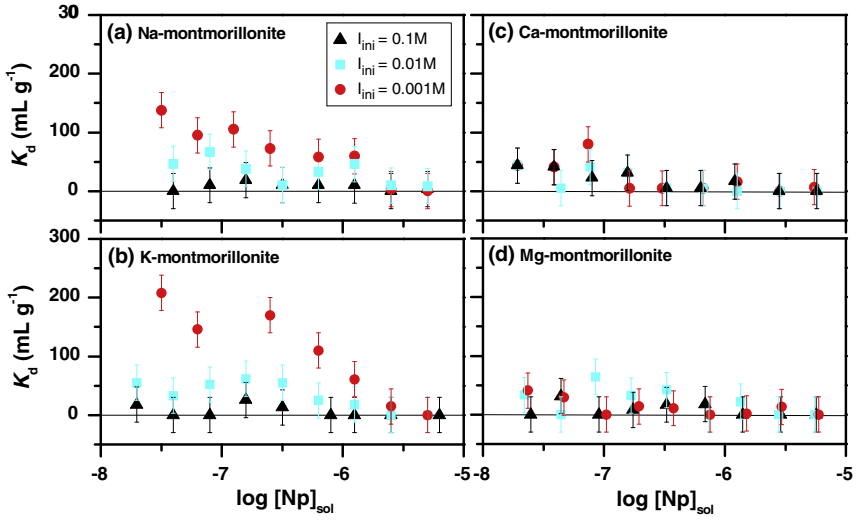

Fig. 3. Np distribution coefficients (K_d) plotted vs. log Np concentration in solution (Np_{sol}) at pH 4.5 and ionic strengths of 0.001 M, 0.01 M and 0.1 M. Errors calculated from 2 S% LSC uncertainties.

Information for all data and uncertainties). In principle, data fitting could be performed such that selectivity coefficients, written as binary reactions, are allowed to vary simultaneously to reach a "best fit". However, in reality, this approach leads to a poorly constrained problem. In addition, this approach leads to an unintended fitting of selectivity coefficients between the major cations (e.g. ${}^{K^+}_{Na^+}K$, etc.) for which simple binary one-site selectivity coefficients are well established in the literature. For example, if the data fitting yields $\log\left({}^{NpO_2^+}_{Na^+}K_V\right)$ and l $\log\left({}^{NpO_2^+}_{K^+}K_V\right)$ selectivity coefficients of −0.34 and −0.31, respectively, it implies a $\log\left({}^{Na^+}_{K^+}K_V\right)$ selectivity coefficient of (−0.34) − (−0.31) = −0.03. However, this value contradicts the selectivity coefficient reported in the literature ($\log\left({}^{Na^+}_{K^+}K_V\right) = 0.26$ (Fletcher and Sposito, 1989)). To minimize the number of fitting parameters in our modeling effort and to ensure consistency with published ion exchange selectivity coefficients between the major cations (i.e. ${}^{K^+}_{Na^+}K$, ${}^{Ca^{2+}}_{Na^+}K$ and ${}^{Mg^{2+}}_{Na^+}K$), we limited our fitting parameter to ${}^{NpO_2^+}_{Na^+}K$ while forcing the ion exchange selectivity coefficients between Np and the other major cations to be determined based on the major cation selectivity coefficients reported in the literature $\left(\text{e.g. } \log\left({}^{NpO_2^+}_{K^+}K_V\right) = \log\left({}^{NpO_2^+}_{Na^+}K_V\right) - \log\left({}^{NpO_2^+}_{K^+}K_V\right)\right)$.

A comprehensive table of Vanselow selectivity coefficients for many major and minor cations (but not Np) and montmorillonite was published by Fletcher and Sposito (1989). The relevant selectivity coefficients used in the present modeling effort are reproduced in Table 1. Note that reactions with clay edges as proposed by Fletcher and Sposito (1989) were not included in this analysis as they were found to be insignificant at the low pH values examined here.

A number of publications by Bradbury and Baeyens have applied the Gaines–Thomas convention to various cation ion exchange datasets (Baeyens and Bradbury, 1995, 1997; Bradbury and Baeyens, 1995, 1997). In these models, the selectivity coefficient, $\log\left({}^{Ca^{2+}}_{Na^+}K_{GT}\right)$, was reported as 0.61. A $\log\left({}^{Mg^{2+}}_{Na^+}K_{GT}\right)$ selectivity coefficient was not reported. However, based on results from Fletcher and Sposito (1989), we assume that the Gaines–Thomas selectivity coefficient for Mg–Na ion exchange will be similar if not equivalent to Ca–Na. For homovalent ion exchange, the Vanselow and Gaines–Thomas conventions are equivalent. Thus, we can use the ${}^{K^+}_{Na^+}K$ value of Fletcher and Sposito (1989) in a Gaines–Thomas model without incurring any additional uncertainty (Table 1).

Importantly, all calculated ion exchange reaction constants contain some level of uncertainty. These uncertainties are a combination of measurement uncertainty and uncertainty associated with the choice of conceptual and numerical model. For example, Tournassat et al. (2011) determined that clay tactoid size and organization will affect the apparent ion exchange properties of clays. In addition, the composition of montmorillonites from different sources can lead to differences in measured ion exchange properties. These effects are not addressed in the present modeling effort. However, it is acknowledged that the resulting Np selectivity coefficients are affected by our choice of a relatively simple one site ion exchange conceptual model.

All data were fit simultaneously while allowing only the ${}^{NpO_2^+}_{Na^+}K$ selectivity coefficient to vary. All other coefficients were taken from Table 1 and a cation exchange capacity for SWy-2 of 764 meq kg^{-1} was used (value reported by the *CMS*). Both the Vanselow and Gaines–Thomas conventions were tested. The resulting constants are listed in Table 2.

The $\log\left({}^{NpO_2^+}_{Na^+}K\right)$ selectivity coefficients based on the Vanselow and Gaines–Thomas conventions are -0.20 ± 0.03 and -0.082 ± 0.04, respectively. The Np(V) selectivity coefficients with respect to K^+, Ca^{2+} and Mg^{2+} were determined (Table 2) based on the fitted ${}^{NpO_2^+}_{Na^+}K$ selectivity coefficient and the fixed major cation selectivity coefficients reported in Table 1. The ${}^{NpO_2^+}_{Na^+}K$ selectivity coefficients determined using the Vanselow and Gaines–Thomas conventions are similar, as would be expected for homovalent exchange reactions. They are also within the range of selectivity coefficients reported in or derived from previous studies for Np–Na ion exchange on smectite ($\log\left({}^{NpO_2^+}_{Na^+}K\right) = 0.06$ to -0.75; values taken or derived from data in Bradbury and Baeyens, 2006; Gorgeon, 1994; Kozai et al., 1996, 1993; Turner et al., 1998 and Zavarin et al., 2012, see Supporting Information Table 6). The difference in Vanselow and Gaines–Thomas selectivity coefficients is caused primarily by the differences in the fixed ${}^{K^+}_{Na^+}K$, ${}^{Ca^{2+}}_{Na^+}K$ and ${}^{Mg^{2+}}_{Na^+}K$) selectivity coefficients used in the two models as shown in Table 1. Residual errors reported in the FIT4FD code as WSOS/DF (weighted sum of squares divided by the degrees of freedom) (Zavarin et al., 2005) were 2.48 using the Vanselow convention and 2.54 using the Gaines–Thomas convention, indicating a very small improvement in the fit to the experimental data with the Vanselow convention.

Fig. 4 compares the Np isotherm data (K_d vs. Np concentration in solution) to the predicted values using the Vanselow fitted $\log\left({}^{NpO_2^+}_{Na^+}K_V\right)$ selectivity coefficient (−0.20) and associated values from Table 1. Given the low Np sorption in the divalent cation systems, values for corresponding Ca^{2+} and Mg^{2+} systems are presented together in the same plot. Fig. 4 shows that a single ${}^{NpO_2^+}_{Na^+}K_V$ fitted selectivity coefficient is able to predict Np(V) sorption to montmorillonite fairly well over the wide range of solution conditions considered in this study.

3.5. Simulation of Np(V) sorption on montmorillonite

In order to illustrate the independent effect of each major cation (Na^+, K^+, Ca^{2+} or Mg^{2+}) on Np ion exchange on montmorillonite without interference from other cations in the electrolyte, Np sorption in mono-electrolyte solutions was simulated using the Vanselow ion exchange model developed above (Table 1). Fig. 5 shows the predicted K_d values over a range of cation concentrations (0.0001–1 M). At equivalent electrolyte cation concentration, Np sorption is lower in divalent systems (Ca^{2+} and Mg^{2+}) than in monovalent systems (K^+ and Na^+). Further, the slope of the curves is lower in divalent systems, as expected of sorption by ionic exchange and as deduced from Eq. (5). Thus, for a homovalent exchange (NpO_2^+–Na^+ or NpO_2^+–K^+) the dependence of the logarithm

Table 1
Reaction constants for Na, K, Ca, and Mg ion exchange on montmorillonite based on the Vanselow and Gaines–Thomas conventions.

Reaction	Log K_V[a]	Log K_{GT}[b]
Mont(Na) + H^+ ↔ Mont(K) + H^+	0.10	0.10[c]
Mont(Na) + K^+ ↔ Mont(K) + Na^+	0.26	0.26[c]
2 Mont(Na) + Ca^{2+} ↔ Mont(Ca) + 2 Na^+	0.17	0.61
2 Mont(Na) + Mg^{2+} ↔ Mont(Mg) + 2 Na^+	0.17	0.61[d]
Mont(Na) + Ca^{2+} + Cl^- ↔ Mont(CaCl) + Na^+	2.28	2.28[c]
Mont(Na) + Mg^{2+} + Cl^- ↔ Mont(MgCl) + Na^+	2.26	2.26[c]

[a] Fletcher and Sposito (1989). K_a is equal to the Vanselow conditional equilibrium constant, K_V, assuming ideal mixing (i.e. activity coefficients for species on the solid phase are equal to one).
[b] Bradbury and Baeyens (1995).
[c] Based on $K_V = K_{GT}$ for homovalent ion exchange.
[d] Assumed based on similar reaction constant reported for Ca^{2+} and Mg^{2+} in the Vanselow model.

Table 2
Fitted ion exchange reaction constants for Np(V).

N° free parameters		Vanselow		Gaines–Thomas	
		log K_V	WSOS/DF[a]	log K_{GT}	WSOS/DF
1	Np–Na	−0.20 (0.03)[b]	2.48	−0.082 (0.04)	2.54
	Np–K[c]	−0.46		−0.34	
	Np–Ca[c]	−0.57		−0.74	
	Np–Mg[c]	−0.57		−0.74	

[a] WSOS/DF means weighted sum of squares divided by the degrees of freedom.
[b] Values in parentheses are the uncertainties in the reported values (at one standard deviation).
[c] Selectivity coefficients calculated from fitted Np–Na selectivity coefficient combined with fixed major cation selectivity coefficients.

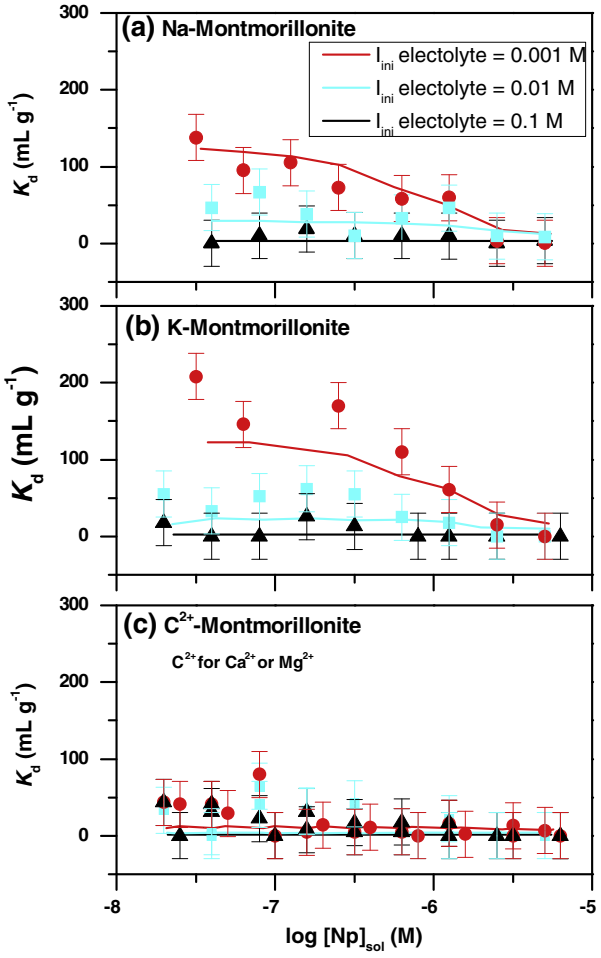

Fig. 4. Experimental data (K_d) and model fit of Np(V) ion exchange (pH 4.5). Predicted values based on the Vanselow convention, using parameters in Table 1 and fitted $\log\left(^{NpO_2^+}_{Na^+}K_V\right) = -0.20$. Errors calculated from 2 S% LSC uncertainties.

of the distribution coefficients ($\log(K_d)$) with the logarithm of the concentration of the main ion of the electrolyte $\log[A]$ is represented by a line with a slope of −1. For NpO_2^+–Ca^{2+} or NpO_2^+–Mg^{2+} exchange, this dependence is a line with slope −0.5, as indicated by the simulation (Fig. 5).

A result of the dependency of Np-montmorillonite exchange on cation concentration shown in Fig. 5, is that high K_d values could be reached in waters with low Na^+ and K^+ concentrations and in the absence of divalent cations. For example, in waters with [Na] or [K] of 10^{-4} M, K_d values of 3800 mL g^{-1} and 2400 mL^{-1} may be achieved. However, such conditions are not characteristic of typical natural waters.

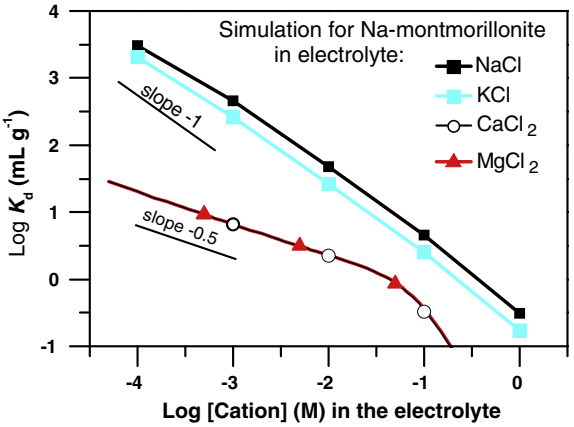

Fig. 5. Simulation of Np(V) ion exchange on montmorillonite (2 g L^{-1}) at pH 4.5 in pure electrolyte (NaCl, KCl, $MgCl_2$ and $CaCl_2$) for $[Np]_{total} = 5 \times 10^{-7}$ M. Predicted values are derived using the Vanselow convention and parameters in Table 1 with fitted $\log\left(^{NpO_2^+}_{Na^+}K_V\right) = -0.20$.

3.6. Predicting Np(V) behavior in natural environments

By taking cation content information for a range of natural waters (assuming Cl^- as the electrolyte anion) (Bajo et al., 1988; Banwart, 1995; Drever, 1997), it was possible to make predictions of Np(V)-montmorillonite permanent charge site ion exchange K_d values in these natural waters for $[NpO_2^+] = 5 \times 10^{-7}$ M (Fig. 6). As ion exchange on such sites is independent of pH, the calculated values are valid for the pH range of these waters. The aim of this effort was to highlight natural scenarios where ion exchange might be expected to play a significant role in Np sorption.

The highest ion exchange derived K_d values were predicted for rainwater (water number 1: $K_d = 48.1$ mL g^{-1}) and streams draining igneous rocks (water number 3: $K_d = 31.3$ mL g^{-1}) which contain Na, K, Na and Ca concentrations lower than 5×10^{-5} M. In contrast, the Np(V)-montmorillonite ion exchange K_d value in seawater (water number 4) is predicted to be zero given the high salinity. The Np(V)-montmorillonite ion exchange K_d values in groundwater (water numbers 5, 6, 7, 8, 9, 10) vary between these end member values as a result of variations in their major cation composition caused by differences in associated bedrock, residence time, or sea water intrusion. In general, for the same cation concentration, divalent cations in waters affect Np(V) exchange on montmorillonite more strongly than monovalent cations. For example, the K_d predicted in groundwater from volcanic rock and from the Sierra Nevada Mountains (USA) (water numbers 6 and 7) are similar (16 and 22 mL g^{-1}, respectively), despite there being an order of magnitude change in monovalent cations concentration. In contrast, when the difference in divalent cation concentration is an order of magnitude, as is the case for waters number 5 and 6, the respective K_d's are 16 mL g^{-1} for water number 6 and 3 mL g^{-1} for water number 5.

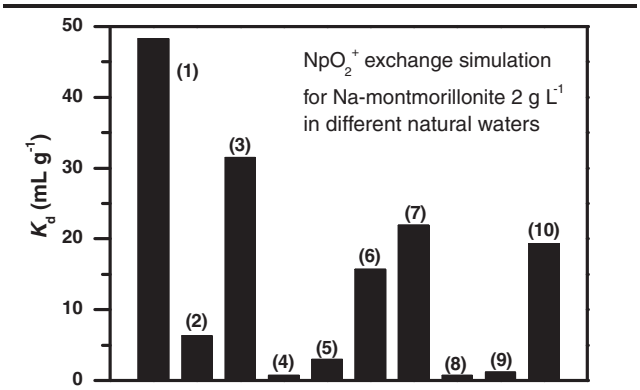

Cation concentration in solution (M)

	Na	K	Σ C^{+} *	Ca	Mg	Σ C^{2+} *
(1)	2.4 E-5	2.8 E-6	2.7 E-5	1.6 E-5	5.8 E-6	2.2 E-5
(2)	6.1 E-5	3.1 E-5	9.2 E-5	1.0 E-3	3.0 E-4	1.3 E-3
(3)	7.0 E-6	7.9 E-6	1.5 E-5	4.2 E-5	9.9 E-6	5.2 E-5
(4)	4.6 E-1	9.7 E-3	4.7 E-1	10.0 E-3	5.6 E-2	6.6 E-2
(5)	1.2 E-3	5.1 E-5	1.2 E-3	3.6 E-3	2.3 E-3	5.9 E-3
(6)	1.6 E-3	7.7 E-5	1.7 E-3	1.6 E-4	4.5 E-5	2.1 E-4
(7)	1.3 E-4	2.8 E-5	1.6 E-4	7.8 E-5	2.9 E-5	1.1 E-4
(8)	1.2 E-1	8.2 E-4	1.2 E-1	1.1 E-1	6.6 E-3	1.2 E-1
(9)	9.1 E-2	2.0 E-4	9.2 E-2	4.2 E-2	1.7 E-3	4.4 E-2
(10)	6.8 E-4	4.0 E-6	6.9 E-4	1.4 E-4	8.0 E-7	1.4 E-4

(1) Average rainwater from sites in North Carolina and Virginia; **(2)** Composition of the Rhine River as it leaves the Alps; **(3)** Stream draining igneous rocks in the Washington Cascades **(4)** Average seawater; **(5)** Groundwater from limestone of the Supai Formation, Grand Canyon; **(6)** Groundwater from volcanic rocks, New Mexico; **(7)** Groundwater from a spring, Sierra Nevada Mountains (USA): short residence time; **(8)** Groundwater from metamorphic rocks in Canada: long residence time; **(9)** Groundwater from granitic site Äspo (Sweden); **(10)** Groundwater from granitic site Grimsel (Switzerland).

(1,2,3,4,5,6,7 and 8) natural water composition from Drever (1997); (9 and 10) from Bajo et al. (1988) and Banwart (1995) * Σ C^{+} refers to sum of Na and K concentration and Σ C^{2+} refers to sum of Ca and Mg concentration

Fig. 6. Composition of representative fresh natural waters and simulation of Np(V) ion exchange on montmorillonite (2 g L^{-1}) for $[Np]_{total} = 5 \times 10^{-7}$ M (Cl^- was the considered electrolyte anion). Predicted values are derived using the Vanselow convention and parameters in Table 1 with fitted $\log \left(\frac{NpO_2^+}{Na^+} K_V\right) = -0.20$.

It should be stressed that in these simulations (Figs. 5 and 6) the intent was to focus solely on the permanent charge site ion exchange component. As a result, the contribution of surface complexation reactions to the overall K_d was not addressed. Turner et al. (1998) predicted K_d values much higher than 50 mL g^{-1} (maximum value predicted in this study in rainwater, Fig. 6) at pH > 7.5, where surface complexation can play an important role. For a true estimation of total Np sorption (ion exchange on all possible sites and surface complexation) the pH, anion composition, and redox conditions must also be taken into account.

However, it can be concluded that Np(V) ion exchange at permanent charge sites could be a relevant mechanism in neutral to acidic pHs and low divalent cation concentration groundwaters.

4. Conclusions

In this study we have shown that Np permanent charge site ion exchange is highly dependent on the major cation composition of the aqueous system, being especially limited by the presence of divalent cations such as Ca^{2+} and Mg^{2+} in solution. In many geochemical systems under medium-acid pH conditions, Np(V) migration-retention will likely be strongly influenced by NpO_2^+ ion exchange on montmorillonite. In neutral to basic groundwater conditions, ionic exchange becomes less significant to the total Np(V) sorption and surface complexation of Np(V) will likely dominate making understanding this process highly valuable.

A sorption model was developed on the basis of the experimental data and on the selectivity coefficients reported in the literature for the exchange between major cations on montmorillonite. The recommended selectivity coefficients for Np(V) ionic exchange on montmorillonite, according to the Vanselow convention, are as follows: $\log \left(\frac{NpO_2^+}{Na^+} K_V\right) = -0.20, \log \left(\frac{NpO_2^+}{K^+} K_V\right) = -0.46, \log \left(\frac{NpO_2^+}{Ca^{2+}} K_V\right) = -0.57, \log \left(\frac{NpO_2^+}{Mg^{2+}} K_V\right) = -0.57$. Their use in geochemical computer codes will allow better predictions of Np(V) behavior in the environment.

From the experimental data and the estimated selectivity coefficients in this study, we can conclude that low salinity natural water, low in divalent cations (Ca^{2+} and Mg^{2+}), favors NpO_2^+ sorption by ion exchange on montmorillonite. In contrast, Np(V) ion exchange will be greatly supressed as divalent cation concentration increases towards millimolar values.

Acknowledgements

This work was supported by the Used Fuel Disposition Campaign of the Department of Energy's Nuclear Energy Program and by the Subsurface Biogeochemical Research Program of the U.S. Department of Energy's Office of Biological and Environmental Research. Prepared by LLNL under Contract DE-AC52-07NA27344 and partially supported by the Spanish Ministry of Economy and Competitiveness under the frame of the NANOBAG Project (CMT2011-27975). A. Benedicto was supported by a Spanish Government 'FPI' pre-doctoral contract (BES-2009-026765). We thank three anonymous reviewers whose comments greatly improved this manuscript.

Appendix A. Supplementary material

Supplementary data associated with this article can be found, in the online version, at http://dx.doi.org/10.1016/j.apgeochem.2014.06.003.

References

Baeyens, B., Bradbury, M.H., 1995. A Quantitative Mechanistic Description of Ni, Zn and Ca Sorption on Na-montmorillonite. Part II: Sorption measurements. PSI Bericht Nr. 95-11 and Nagra Technical Report NTB 95-05, Wettingen and Villigen (Switzerland).

Baeyens, B., Bradbury, M.H., 1997. A mechanistic description of Ni and Zn sorption on Na-montmorillonite.1. Titration and sorption measurements. J. Contam. Hydrol. 27, 199–222.

Baeyens, B., Bradbury, M.H., 2004. Cation exchange capacity measurements on illite using the sodium and cesium isotope dilution technique: effects of the index cation, electrolyte concentration and competition: modeling. Clays Clay Miner. 52, 421–431.

Bajo, C., Hoehn, E., Keil, R., Baeyens, B., 1988. Chemical Characterisation of the Groundwater from the Fault Zone AU 96, NAGRA Technical Report 88–23, Wettingen (Switzerland).

Banwart, S., 1995. The Äspö redox investigations in block scale. Project summary and implications for repository performance assessement. SKB Technical Report 95–26, Stockholm (Sweden).

Benedicto, A., Degueldre, C., Missana, T., 2014. Gallium sorption on montmorillonite and illite colloids: experimental study and modeling by ionic exchange and surface complexation. Appl. Geochem. 40, 43–50.

Bethke, C.M., Yeakel, S., 2009. The Geochemist's Workbench. Release 8.0. Essentials Guide.

Bolt, G.H., 1982. Soil Chemistry. B. Physico-Chemical Models. Elsevier (Chapter 2).

Bondietti, E.A., Francis, C.W., 1979. Geologic migration potentials of TC-99 and NP-237. Nature 203, 1337–1340.
Bradbury, M.H., Baeyens, B., 1995. A Quantitative Mechanistic Description of Ni, Zn and Ca Sorption on Na-montmorillonite. Part III: Modelling. PSI Bericht Nr. 95–12 and Nagra Technical Report NTB 95–06, Wettingen and Villigen (Switzerland).
Bradbury, M.H., Baeyens, B., 1997. A mechanistic description of Ni and Zn sorption on Na-montmorillonite Part II: modelling. J. Contam. Hydrol. 27, 223–248.
Bradbury, M.H., Baeyens, B., 2000. A generalised sorption model for the concentration dependent uptake of caesium by argillaceous rocks. J. Contam. Hydrol. 42, 141–163.
Bradbury, M.H., Baeyens, B., 2006. Modelling sorption data for the actinides Am(III), Np(V) and Pa(V) on montmorillonite. Radiochim. Acta 94, 619–625.
Bradbury, M.H., Baeyens, B., 2009. Sorption modelling on illite. Part II: Actinide sorption and linear free energy relationships. Geochim. Cosmochim. Acta 73, 1004–1013.
Cantrell, K.J., 2009. Transuranic Contamination in Sediment and Groundwater at the U.S. DOE Hanford Site (PNNL-18640). Pacific Northwest National Laboratory, Richland, WA.
Choppin, G.R., 2006. Actinide speciation in aquatic systems. Mar. Chem. 99, 83–92.
Dixon, J.B., 1989. Minerals in Soil Environments, second ed. Soil Science Society of America.
Drever, J.I., 1997. The Geochemistry of Natural Waters: Surface and Groundwater Environments. Prentice Hall.
Felmy, A.R., Cantrell, K.J., Conradson, S.D., 2010. Plutonium contamination issues in Hanford soils and sediments: discharges from the Z-Plant (PFP) complex. Phys. Chem. Earth 35, 292–297.
Fletcher, P., Sposito, G., 1989. The chemical modeling of clay electrolyte interactions for montmorillonite. Clay Miner. 24, 375–391.
Gaines, G.L., Thomas, H.C., 1953. Adsorption studies on clay minerals II. A formulation of the thermodynamic of exchange adsorption. J. Chem. Phys. 21, 714–718.
Gorgeon, L., 1994. Contribution à la Modélisation Physico-Chimique de la Retention de Radioéléments à Vie Longue par des Matériaux Argileux, Université Paris.
Hoth, P., Wirth, H., Reinhold, K., Bräuer, V., Krull, P., Feldrappe, H., 2007. Endlagerung radioaktiver Abfälle in tiefen geologischen Formationen Deutschlands – Untersuchung und Bewertung von Tongesteinsformationen. BGR Bundesanstalt für Geowissenschaften und Rohstoffe, Hannover.
Jensen, H.E., 1973. Potassium–calcium exchange equilibria on a montmorillonite and a kaolinite clay. Agrochimica 17, 181–190.
Kaszuba, J.P., Runde, W.H., 1999. The aqueous geochemistry of neptunium: dynamic control of soluble concentrations with applications to nuclear waste disposal. Environ. Sci. Technol. 33, 4427–4433.
Kozai, N., Ohnuki, T., Muraoka, S., 1993. Sorption characteristics of neptunium by sodium-smectite. J. Nucl. Sci. Technol. (Tokyo, Jpn.) 30, 1153–1159.
Kozai, N., Ohnuki, T., Matsumoto, J., Banba, T., Ito, Y., 1996. A study of specific sorption of neptunium(V) on smectite in low pH solution. Radiochim. Acta 75, 149–158.
Langmuir, D., 1997. Aqueous Environmental Geochemistry. Prentice-Hall, U.S.
Law, G.T.W., Geissler, A., Lloyd, J.R., Livens, F.R., Boothman, C., Begg, J.D.C., Denecke, M.A., Rothe, J., Dardenne, K., Burke, I.T., Charnock, J.M., Morris, K., 2010. Geomicrobiological redox cycling of the transuranic element neptunium. Environ. Sci. Technol. 44, 8924–8929.
Lemire, R.J., Fuger, J., Nitsche, H., Potter, P., Rand, M.H., Rydberg, J., Spahiu, K., Sullivan, J.C., Ullman, W.J., Vitorge, P., Wanner, H., 2001. Chemical Thermodynamics of Neptunium and Plutonium. North-Hollande by Elsevier, Amsterdam.
Maes, A., Cremers, A., 1977. Charge density effects in ion exchange. Part 1. Heterovalent exchange equilibria. J. Chem. Soc. Faraday Trans. 173, 1807–1814.
McBride, M.B., 1994. Environmental Chemistry of Soils. Oxford University Press, Oxford.
Mironenko, M.V., Malikov, D.A., Kulyako, Y.M., Myasoedov, B.F., 2006. Sorption of Np(V) on montmorillonite from solutions of $MgCl_2$ and $CaCl_2$. Radiochemistry 48, 69–74.
Missana, T., García-Gutiérrez, M., 2007. Adsorption of bivalent ions (Ca(II), Sr(II) and Co(II)) onto FEBEX bentonite. Phys. Chem. Earth 32, 559–567.
Nagasaki, S., Tanaka, S., 2000. Sorption equilibrium and kinetics of NpO_2^+ on dispersed particles of Na-montmorillonite. Radiochim. Acta 88, 705–709.
NAGRA, 2002. Project Opalinus Clay. Safety Report. Demonstration of disposal feasibility for spent fuel, vitrified high-level waste and long-lived intermediate-level waste (Entsorgungsnachweis). NTB 02-05. Nagra, Wettingen, Switzerland.
Neck, V., Kim, J.I., Kanellakopulos, B., 1994. Thermodynamisches Verhalten von Neptunium(V) in konzentrierten NaCl- und $NaClO_4$-Lösungen, Tech. Rep. Kfk 5301. Kernforschungszentrum Karlsruhe, Karlsruhe, Germany.
OECD, 2006. Safety of Geological Disposal of High-level and Longlived Radioactive Waste in France—an International Peer Review of the "Dossier 2005 Argile" Concerning Disposal in the Callovo-Oxfordian Formation. NEA No. 6178. OECD.
Parkhurst, D.L., Appelo, C.A.J., 1999. User's Guide to Phreeqc—a Computer Program for Speciation, Batch-reaction, One-dimensional Transport, and Inverse Geochemical Calculations, USGS Report No. 99-4259.
Pickett, D.A., Murrell, M.T., Williams, R.W., 1994. Determination of femtogram quantities of protactinium in geologic samples by thermal ionization mass spectrometry. Anal. Chem. 66, 1044–1049.
Poinssot, C., Baeyens, B., Bradbury, M.H., 1999. Experimental Studies of Cs, Sr, Ni and Eu Sorption on Na-illite and the Modelling of Cs Sorption, PSI Bericht Nr. 99-06, pp. 61.
Runde, W., Conradson, S.D., Efurd, D.W., Lu, N., VanPelt, C.E., Tait, C.D., 2002. Solubility and sorption of redox-sensitive radionuclides (Np, Pu) in J-13 water from the Yucca Mountain site: comparison between experiment and theory. Appl. Geochem. 17, 837–853.
Sabodina, M.N., Kalmykov, S.N., Sapozhnikov, Y.A., Zakharova, E.V., 2006. Neptunium, plutonium and Cs-137 sorption by bentonite clays and their speciation in pore waters. J. Radioanal. Nucl. Chem. 270, 349–355.
Sakamoto, Y., Konishi, M., Shirahashi, K., Senoo, M., Moriyama, N., 1990. Adsorption behavior of neptunium for soil. Radioact. Waste Manage. Environ. Restor. 15, 13–25.
Schindler, P.W., Liechti, P., Westall, J.C., 1987. Adsorption of copper, cadmium and lead from aqueous solution to the kaolinite/water interface. Neth. J. Agric. Sci. 35, 219–230.
Shaviv, S., Mattigod, S.V., 1985. Cation exchange equilibria in soils expressed as cation-ligand complex formation. Soil Sci. Soc. Am. J. 49, 569–573.
Smith, D.K., Finnegan, D.L., Bowen, S.M., 2003. An inventory of long-lived radionuclides residual from underground nuclear testing at the Nevada test site, 1951–1992. J. Environ. Radioact. 67, 35–51.
Sposito, G., 1981. The Thermodynamics of Soil Solution. Oxford University Press, Oxford.
Tournassat, C., Gailhanou, H., Crouzet, C., Braibant, G., Gautier, A., Lassin, A., Blanc, P., Gaucher, E.C., 2007. Two cation exchange models for direct and inverse modelling of solution major cation composition in equilibrium with illite surfaces. Geochim. Cosmochim. Acta 71, 1098–1114.
Tournassat, C., Bizi, M., Braibant, G., Crouzet, C., 2011. Influence of montmorillonite tactoid size on Na–Ca cation exchange reactions. J. Colloid Interface Sci. 364, 443–454.
Triay, I.R., Robinson, B.A., Lopez, R.M., Mitchell, A.J., Overly, C.M., 1993. Neptunium retardation with tufts and groundwaters from Yucca Mountain. In: Proc 4th Annu Int Conf on High-Level Radioactive Waste Management. Am. Nuclear Soc., La Grange Park, IL, pp. 1504–1508.
Turner, D.R., Pabalan, R.T., Bertetti, F.P., 1998. Neptunium(V) sorption on montmorillonite: an experimental and surface complexation modeling study. Clays Clay Miner. 46, 256–269.
Waggener, W.C., 1958. Measurement of the absorption spectra of neptunium ions in heavy water solution from 0.35 to 1.85 μ. J. Phys. Chem. 62, 382–383.
Wescott, R.G., Lee, M.P., McCartin, T.J., Eisenberg, N.A., Baca, R.G., 1995. NRC Iterative Performance Assessment Phase 2: Development of Capabilities for Review of a Performance Assessment for a High-level Waste Repository. NUREG-1464. Nuclear Regulatory Commission, Washington, DC.
Wilson, M.L., Gauthier, J.H., Barnard, R.W., Barr, G.E., Dockery, H.A., Dunn, E., Eaton, R.R., Guerin, D.C., Lu, N., Martinez, M.J., Nilson, R., Rautman, C.A., Robey, T.H., Ross, B., Ryder, E.E., Schenker, A.R., Shannon, S.A., Skinner, L.H., Halsey, W.G., Gansemer, J.D., Lewis, L.C., Lamont, A.D., Triay, I.R., Meijer, A., Morris, D.E., 1994. Total-system Performance Assessment for Yucca Mountain–SLN Second Iteration (TSPA-1993). SAND93-2675, vol. 1 and 2. Sandia National Laboratories, Albuquerque.
Yariv, S., Cross, H., 1979. Geochemistry of Coloid Systems for Earth Sciences. Springer-Vergag (Chapter 2).
Zavarin, M., Roberts, S.K., Hakem, N., Sawvel, A.M., Kersting, A.B., 2005. Eu(III), Sm(III), Np(V), Pu(V), and Pu(IV) sorption to calcite. Radiochim. Acta 93, 93–102.
Zavarin, M., Powell, B.A., Bourbin, M., Zhao, P., Kersting, A.B., 2012. Np(V) and Pu(V) ion exchange and surface-mediated reduction mechanisms on montmorillonite. Environ. Sci. Technol. 46, 2692–2698.